Astronomy & Astrophysics manuscript no. cores
March 21, 2017
©ESO 2017

A CS survey of small molecular cores⋆

Bengt Larsson[1] and René Liseau[2]

[1] Stockholm University, AlbaNova University Center, Department of Astronomy, SE-106 91 Stockholm, Sweden, e-mail: bem@astro.su.se
[2] Chalmers University of Technology, Onsala Space Observatory, Department of Earth and Space Sciences, SE-439 92 Onsala, Sweden, e-mail: rene.liseau@chalmers.se

Received ; accepted

arXiv:1703.06462v1 [astro-ph.GA] 19 Mar 2017

ABSTRACT

Context. Stars form in large clusters or in relative solitude, resulting in different mass spectra. Here, we are addressing the sites of isolated low mass star formation in the solar neighbourhood, i.e. small cloud cores within one kiloparsec.
Aims. We aim at determining the physical parameters of the cores, i.e., temperature, volume density, column density and (radial) velocity fields, and the status of star formation.
Methods. Surveying small dark clouds in both celestial hemispheres we study the physical conditions of low-mass star formation for detectable core masses $M \geq 0.01\,M_{\odot}$. The target list is drawn from catalogues of optically selected dark cloud cores, where, the visual extinction exceeds 5 magnitudes ($A_{\rm V}> 5$ mag). The selected probe is the CS molecule that needs high densities for excitation of its rotational levels. To gauge the state of excitation, the cores were observed in two transitions. In a limited number of cases (24), optical depths were derived from complementing lines of the rarer isotopologue $C^{34}S$ for the (2-1) and (3-2) transitions.
Results. Making small maps ($3' \times 3'$) maps, the 471 optically selected cores were searched for CS ($J = 2 \rightarrow 1$) and 315 (67%) were detected ($T_{\rm A}^{\star} \geq 3\sigma$). Similarly, 431 cores were observed in CS ($J = 3 \rightarrow 2$), of which 141 (33%) were clearly detected ($T_{\rm A}^{\star} \geq 3\sigma$). In general, the position of peak CS emission does not coincide with the optically determined centre of the cores.
Conclusions. The cores appear cold ($T < 10$ K) and, in the majority of cases, the CS emission is optically thin ($\tau < 1$). On the arcminute scales of the observations, the median column density of carbon monosulfide is $N({\rm CS}) = 7 \times 10^{12}\,{\rm cm}^{-2}$. For an average abundance of $N({\rm CS})/N({\rm H_2}) = 10^{-8}$, the median mass of the detected cores is $1.0\,M_{\odot}$. The line shapes are most often Gaussian with widths exceeding that due to thermal broadening of $\lesssim 0.1\,{\rm km\,s^{-1}}$. The observed median FWHM = $0.7\,{\rm km\,s^{-1}}$, i.e. non-thermal turbulence contributes dominantly to the line widths.

Key words. ISM: molecules – clouds – evolution – Stars: formation

1. Introduction

Many cold and dense cloud cores in the interstellar medium will eventually evolve towards dynamical instability and form stars. For the cloud contraction to proceed, the generated compressional heat needs to be channeled away. This can be achieved by means of radiation losses through collisionally excited spectral lines. The first major computation of the expected cooling rates in molecular cloud conditions were presented by Goldsmith & Langer (1978). Water vapour (H_2O) was found to be the dominant cooling agent at densities exceeding $10^5\,{\rm cm}^{-3}$, irrespectively of the kinetic temperature of the gas. These early models did not consider the effects of molecular depletion from the gas phase due to freeze-out onto dust grains: during more recent years, observations from space indicated much lower abundances than what had been assumed in the earlier works.

From an observational point of view, such studies require trustworthy statistics and, hence, large homogeneous samples. To identify the dense regions where the water cooling could be expected to become efficient, we selected molecular probes whose critical densities[1] are above $10^5\,{\rm cm}^{-3}$. Being readily excited, the low-J rotational transitions of the relatively abundant carbon monosulfide (CS) seemed a good option.

1.1. Sample selection

The sample of dark cores in the Solar Neighbourhood ($d \leq 1$ kpc) is based on visual selection from the Palomar and ESO/SERC survey plates. The work by Clemens & Barvainis (1988) yielded a large sample of isolated cores (248) in the 'northern' hemisphere ($\delta \geq -33°$), with equatorial coordinates accurate to 30″. For the 'northern' catalogue, these data were complemented with ammonia cores by Benson & Myers (1989), DCO^+ cores in ρ Oph of Loren et al. (1990) and bright-rimmed globules of Sugitani et al. (1991).

Hartley et al. (1996) compiled the 'Lynds' catalogue of the Southern Sky', containing 1101 entries (see also Feitzinger & Stüwe 1985), with equatorial coordinates better than 10″. This list includes Sandqvist's dark clouds (Sandqvist 1977) and Zealey's cometary globules (Zealey et al. 1983). From the catalogue by Hartley et al. (1996), the cores corresponding to those of the 'northern' sample were selected. In particular, the visual extinction $A_{\rm V} \geq 6$ mag ('Density = A', which should equal

⋆ Based on observations with the 12 m NRAO (Kitt Peak, Arizona, USA), the 15 m SEST (ESO, La Silla, Chile) and the 20 m OSO (Onsala, Sweden) millimetre-wave antennae.

[1] The critical density is defined as the density at which radiative and collisional de-excitation rates are equal. At $T \sim 20$ K, $n_{\rm crit} \sim 2 \times 10^5\,{\rm cm}^{-3}$ for CS (2-1) and $1 \times 10^6\,{\rm cm}^{-3}$ for (3-2).

Lynds' highest opacity classes = 5 and 6). The core size was initially set not to exceed 10′, but this effective radius was redefined to be at most 4′ (see: Clemens & Barvainis 1988). Here, the size is defined as $r_{\rm eff} = \sqrt{a \times b}$ with the semiaxes of the source ellipse in arcminutes. This procedure could be expected to ensure a volume limited sample, since the number of foreground stars $N_{\rm star}$ is small and the distance D to dark clouds is proportional to $N_{\rm star}$, e.g. $d = 320\,N_{\rm star}^{0.57}$ pc over a 5′ sky area (Herbst & Sawyer 1981). The resulting 'southern' catalogue contained 193 cores.

All in all, the initial target list ('northern' + 'southern') contained 538 objects. The majority of observed dense cores has a distinctly non-spherical geometry. Typical aspect ratios are of the order of 2:1 (see, e.g., Hartley et al. 1996, Clemens & Barvainis 1988, Benson & Myers 1989).

1.2. Distribution of the cores in the sky

Not entirely unexpected, the majority of cores is found in, or relatively close to, the galactic plane (Fig. 1), where the high density of background stars provides a high contrast for the dark globules. Comparing the LSR-velocities of the core gas with models of the galactic rotation indicates that most of the cores are within 1 kpc from the Sun, i.e. that they indeed belong to the Solar Neighbourhood ($|\upsilon_{\rm lsr}| \lesssim 10\,{\rm km\,s^{-1}}$).

1.3. Mass sensitivity of the core survey

We adopted a limiting antenna temperature of 20 mK (averaged over the 9-point map, cf. Sect. 3) or 60 mK (for any individual position) in the CS (2-1) line. This sensitivity corresponds roughly to a limiting LTE column density [2] $N({\rm CS}) = (3-5) \times 10^{11}\,{\rm cm^{-2}}$. For a CS abundance relative to H_2, $X({\rm CS}) = 1 \times 10^{-8}$ (Irvine et al. 1987), this would correspond to a hydrogen column $N(H_2)$ = a few $\times\, 10^{19}\,{\rm cm^{-2}}$. This limit is much smaller than the expected column densities of the molecular gas associated with the high dust extinction (several $A_{\rm V}$) through the centres of the cores, since (on the average) $N(H_2) = 0.94{\times}10^{21}\,A_{\rm V}\,{\rm cm^{-2}\,mag^{-1}}$ (2).

At the distance of 500 pc, an object 1′ in size (the approximate size of the telescope beam), i.e. with diameter of 0.145 pc, the minimum detectable mass would thus be of the order of $10^{-2}\,M_\odot$. Likely effects due to subthermal excitation, line opacity, low beam filling and/or convolutedness of the object could increase this number to a higher value. However, the survey should be sensitive to the standard scale of star formation, viz. the Jeans-mass (Jeans 1927). For a of a cloud of ideal gas, $M_{\rm Jeans} = 0.57 \left(\frac{T}{10\,{\rm K}}\right)^{\frac{3}{2}} \left(\frac{n({\rm H_2})}{10^5\,{\rm cm^{-3}}}\right)^{-\frac{1}{2}} M_\odot$. The numerical constant assumes the mean molecular weight $\mu = 2.4$ for metal rich, fully molecular gas. A cloud of mass larger than $M_{\rm Jeans}$ will be prone to gravitational collapse on a free-fall time scale $t_{\rm ff} = 1.0 \times 10^5 \left(\frac{n({\rm H_2})}{10^5\,{\rm cm^{-3}}}\right)^{-\frac{1}{2}}$ yr. In real, rotating clouds, various pressure gradient forces, including magnetic field stresses, will potentially prolong this time scale by factors of several (e.g., Ciolek & Mouschovias 1995). The matter will fall freely toward the centre of mass with a velocity $\upsilon_{\rm ff} = 0.20 \left(\frac{M}{1\,M_\odot}\right)^{\frac{1}{2}} \left(\frac{R}{0.1\,{\rm pc}}\right)^{-\frac{1}{2}}\,{\rm km\,s^{-1}}$.

2. Observations and data reduction

During several observing runs in 1996 and 1997, we exploited three different observatories, viz. the National Radio Astronomy Observatory (NRAO), Kitt Peak, Arizona, USA, the Onsala Space Observatory (OSO), Onsala, Sweden, and the European Southern Observatory, La Silla, Chile. There, we used the single-dish antennae of 12 m, 20 m and 15 m diameter, respectively. The La Silla telescope is a Swedish-ESO joint facility, i.e. the Swedish ESO Submillimetre Telescope (SEST).

The pointing accuracy of the SEST and OSO 20 m was regularly checked using SiO maser stars as references and was found to be about 4″ (rms). The planets Jupiter and Saturn were used for the NRAO 12 m telescope, resulting in an accuracy of 8″ (rms). From the observation of overlapping sources we determined the 3-telescope inter-calibration for the various transitions to be within 15%–20%.

The CS (2-1) and (3-2), i.e. short-hand for $^{12}C^{32}S$ ($J \rightarrow J-1$), transitions (and their isotopic lines, see Table 1) could be observed simultaneously at the SEST, whereas for the northern sources these observations were split between OSO and Kitt Peak, cf. Table 2. SIS-mixer receivers were used as front-ends at all telescopes, whereas as back-ends we used Autocorrelators, Hybrid Autocorrelators (AC, HAC) and Acousto-optical spectrometers (AOS).

All observations were done in frequency switching mode, with switch frequencies of 4 MHz and 6 MHz (about 8 to $18\,{\rm km\,s^{-1}}$). Standard reductions included the removal of artefacts (interference spikes), the folding of the spectra and the polynomial fitting of the baseline and its removal. Finally, the properly weighted data were averaged to generate one spectrum per line and per position.

Integration times were typically of the order of 60 s per position. For each source, and for each line, a 3×3 map was obtained, aligned with the equatorial coordinate system and with 60″ spacings. This was a trade-off between an acceptable sampling rate and a sufficient sky coverage within the available observing time. These small maps should give us a hint at the degree of compactness of the CS emission.

3. Results

3.1. CS (2-1) and CS (3-2) detection rates

Of the originally selected sources, 471 (88%) were observed in CS (2-1) and 431 (80%) in CS (3-2). Table 5 summarises the observational results. Detections at the $\geq 3\sigma$ level of the antenna temperature $T_{\rm A}^\star$ were two thirds (315) in the (2-1) and one third (141) in the (3-2) transition. These relatively high detection rates clearly support the view that the selected dark dust patches in the sky are sites of high molecular gas density, approaching those of the critical values of the CS transitions.

3.2. Line intensities and line widths

Limiting the sample to cores with $|\upsilon_{\rm LSR}| < 20\,{\rm km\,s^{-1}}$ results in the distributions[3] for 283 CS (2-1) sources shown in Fig. 2. The median line intensity is $\int T_{\rm mb} d\upsilon = 0.6\,{\rm K\,km\,s^{-1}}$ and the observed

[2] This assumes kinetic temperatures in the range (10-30) K, line widths of $\sim 0.7\,{\rm km\,s^{-1}}$, unit beam filling and a main beam efficiency of 70%.

[3] Note regarding all distribution plots: Each bin is the average of 10 different samplings of the data. The bin size is kept constant, but the mid point of the bin is shifted by 10% of the bin size for each of the 10 samplings. The error bars represent $\pm\sqrt{\sigma_S^2 + \sigma_N^2}$ where σ_S is the mean

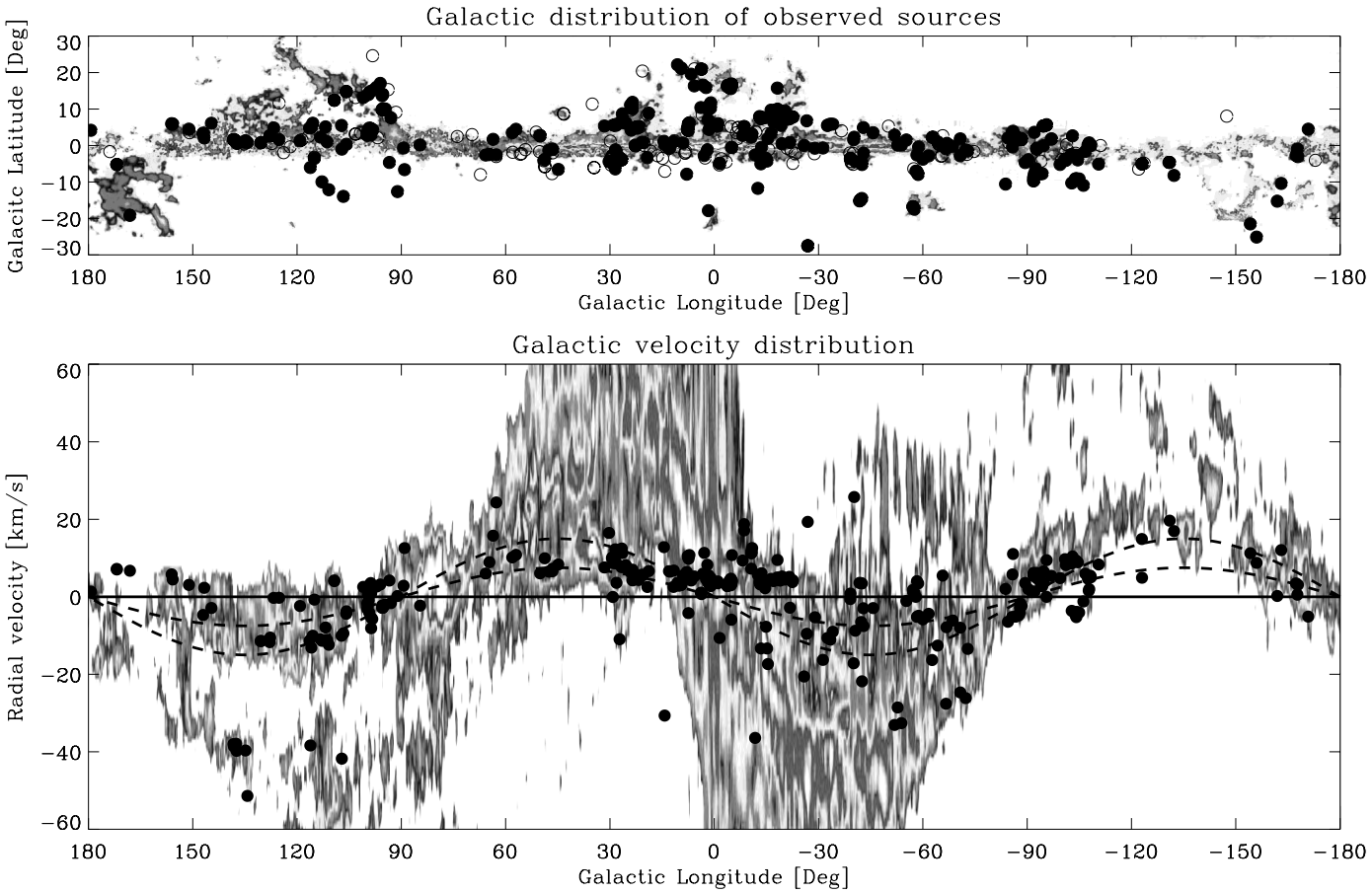

Fig. 1. Small dark cloud cores are shown on maps of the large scale CO (1-0) distribution in the Galaxy (6). **Upper panel:** The sky distribution of the cores observed in rotational transitions of CS. The filled circles represent detections in CS (2-1), for which $T_{\rm A}^{\star} \geq 3\sigma$. **Lower panel:** The spatial LSR-velocity distribution of these detected cores. A simple Oort-type model is shown by the dashed lines to guide the eye, corresponding to distances of 0.5 kpc and 1.0 kpc, respectively. Formally, these loci are given by $\upsilon_{\rm lsr} = 13\,d\,\sin 2\,\ell$, where d is the distance in kpc and ℓ is the galactic longitude.

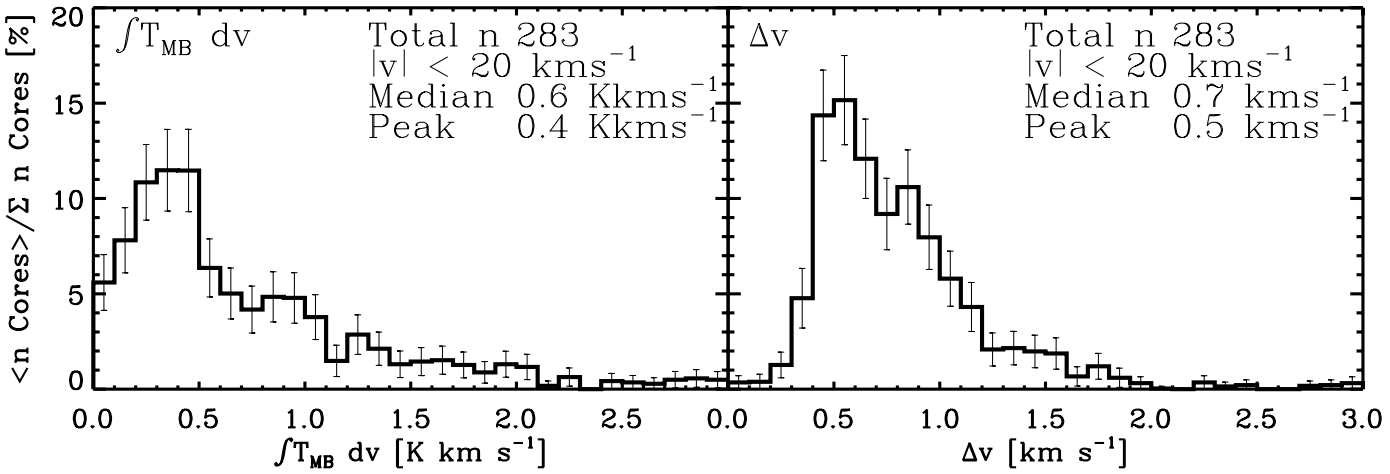

Fig. 2. *Left*: The distribution of integrated CS (2-1) line intensity toward cores, the LSR-velocity of which fall in the interval $-20 < \upsilon_{\rm lsr} < 20$ km s^{-1}. *Right*: The CS (2-1) line width distribution for these cores.

median line width is FWHM = 0.7 km s^{-1}. That this result is not limited by the resolution of the spectrometers is verified in Fig. 3, where similar distributions are shown for objects for which both valid ($T_{\rm A}^{\star} > 3\sigma$) CS (2-1) and CS (3-2) data are available (132 sources), since the higher frequency lines provide a better velocity resolution (cf. Table 2).

These observed line widths are much larger than those from purely thermal broadening, viz. $\upsilon_{\rm th} = 0.06\,\sqrt{T/(10\,{\rm K})}$ km s^{-1}, and are thus dominated by other types of motion, including non-thermal turbulence.

error of that average and σ_N is the square root of the number of cores in that bin.

Table 1. Rotational transitions in carbon monosulfide

Parameter	Transition CS (2 − 1)/$C^{34}S$ (2 − 1)	CS (3 − 2)/$C^{34}S$ (3 − 2)
Tuning frequency setting ν_0 [MHz]	97980.968/96412.982	146969.049/144617.147
Wavelength of transition [mm]	3.06/3.11	2. 04/2.07
Energy above ground $\Delta E_u/k$ [K]	7.05 /6.94	14.11/13.88
Radiative transition rate[a] A_{ul} [s^{-1}]	$1.675 \times 10^{-5}/1.596 \times 10^{-5}$	$6.055 \times 10^{-5}/5.771 \times 10^{-5}$
Collision constant[b] γ_{ul}(20 K) [$cm^3\ s^{-1}$]	6.96×10^{-11}	4.70×10^{-11}
Critical density n_{crit}(20 K) [cm^{-3}]	2.4×10^5	1.3×10^6

[a] see also: Pineiro et al. (1987), Chandra et al. (1995).
[b] Turner et al. (1992).

Table 2. Millimetre wave observatories

Parameter	Telescope/Transition 20 m OSO CS (2 − 1)	12 m NRAO (3 − 2)	15 m SEST (2 − 1)	15 m SEST (3 − 2)
Observing run	Jan 97, Mar 97	May 97, Jun 97	Oct 96, Jun 97	Oct 96, Jun 97
Beam size (HPBW) [″]	37	41	50	33
Main beam efficency η_{mb}	0.56	0.55	0.70	0.66
T_{sys} [K]	390	270	160	190
Frequency Throw [MHz]	6	4	4	4
Spectrometer[a]	AC	HAC	AOS	AOS
Bandwidth [MHz]	80	37.5	43	43
Number of channels	1600	768	1000	1000
Resolution, $\Delta\upsilon$ [km s^{-1}]	0.31	0.20	0.26	0.18
$T_A^\star$ (rms) [mK $channel^{-1}$]	89	67	68	79

[a] AC = AutoCorrelator, HAC = Hybrid AutoCorrelator, AOS = AcoustoOptical Spectrometer.

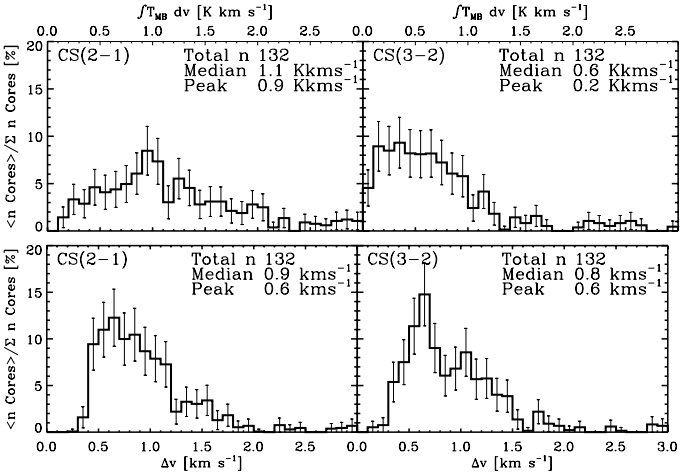

Fig. 3. Same as in Fig. 2 but for a reduced sample where both CS (2-1) and CS (3-2) lines were detected and for which the LSR- velocity $-20 < \upsilon_{lsr} < 20$ km s^{-1}. *Left*: CS (2-1) and *Right*: CS (3-2).

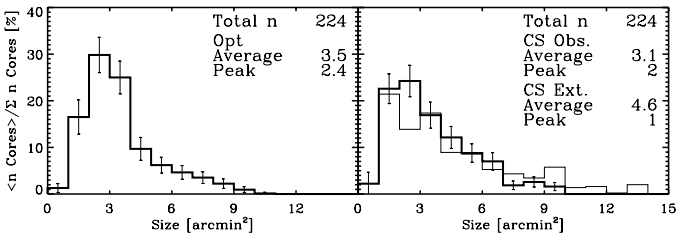

Fig. 4. The source size distribution. *Left panel*: The optically estimated size (from the source catalogues). *Right panel*: The size from the CS (2-1) observations, where the observed maps are represented by the thick line, whereas the thin line depicts the extended distribution (see the text).

3.3. Positional coincidences and source sizes

As described in the previous section, 9-point maps ($3' \times 3'$) were obtained for each core. Inspection of these small maps (Table 5) reveals that the CS (2-1) peak emission most often does not coincide with the optically determined centre position. The fraction of sources for which positional agreement exists amounts to 38%. One explanation could be that the molecular line observations better probe the regions of maximum density (core centre) than the optical data which saturate at $A_V \sim 5$ mag, i.e., becoming indiscriminant for higher opacity regions.

In Fig. 4, the optically determined core sizes and those found from the CS (2-1) observations are shown. The selection is biased and the CS mapping incomplete. However, from the figure it is evident that the sample is peaked towards small CS cores with an average value of 3.1 $arcmin^2$. Even though the observed map is small and under-sampled, one can still get a rough estimate of the core extent in CS, simply by adding the number of map positions, each 1 $arcmin^2$ in size, where the detected signal is larger than half the peak intensity.

As already mentioned, the peak intensity of the CS line is not always found at the centre position. In addition, several cores show evidence of being extended on scales larger than our limited maps. We will therefore potentially underestimate the sizes of a number of cores. By assuming that the core is symmetric

Fig. 5. Examples of mirroring the observed maps of extended sources (large dots symbolise peak integrated line emission, whereas the smaller symbols refer to those positions where the emission is above 50% of the peak value). *Left*: The peak is at a map edge. *Right*: The peak is in a map corner.

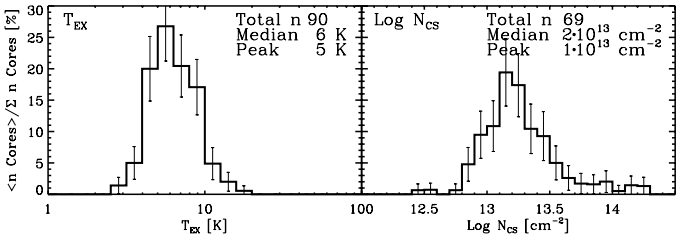

Fig. 6. *Left*: Excitation temperatures derived from the two transitions of CS (2-1) and CS (3-2), under the assumption of low line opacities. *Right*: The CS column densities derived from these transitions. For both distributions, the parameters are larger than 3σ, resulting in different total numbers.

around its peak and by mirroring the map with respect to this position, a somewhat better estimate of the source size can be found (see Fig. 5 for examples).

Finally, the resulting size distribution is also shown in Fig. 4. The average core size is about (4 ± 1) arcmin^2 (optical: 3.5 ± 0.2, CS (2-1): 3.1 ± 0.2, extrapolated CS: 4.6 ± 0.3). These independent size estimates (optical and CS) are in good agreement, indicative of a tight relation between the dust and the molecular gas (the average size ratio $\log[\text{Optical/CS}\,(2-1)] = -0.085$, with a variance of 0.092). This indicates that, on the average, the beam should to a large extent be filled around the peak position.

3.4. The volume limited sample

The number of cores N subtending a given solid angle Ω can be written as $\frac{dN}{d\Omega} = \frac{dN}{dD}\frac{dD}{d\Omega}$, where D is the distance to the core. For the case that the cores are of the same size and are evenly distributed in space, the following applies $\frac{dN}{dD} \propto \Omega^{-1}$ and that $\frac{dD}{d\Omega} \propto \Omega^{-3/2}$. This integrates to $N(\Omega) \propto \Omega^{-3/2}$, so that the slope of this distribution is $\frac{d\log N}{d\log\Omega} = -1.5$.

The core size distributions of Fig. 4 all have slopes of about -1.5, consistent with the result of Eq. 12 (optical: -1.62 ± 0.4, CS (2-1): -1.26 ± 0.28, extrapolated CS: -1.28 ± 0.16). We take this to support our view that the selected core sample is reasonably homogeneous and volume limited.

4. Discussion

4.1. Optically thin emission: $C^{34}S$ (2-1) and $C^{34}S$ (3-2)

The solution to the equation of radiative transfer of molecular radio lines reads $T = f_{\rm beam}\left[\mathcal{F}(T_{\rm ex}) - \mathcal{F}(T_{\rm bg})\right](1 - e^{-\tau})$, where $\mathcal{F}(T) = \frac{h\nu/k}{e^{h\nu/kT}-1}$ and the symbols have their usual meaning. $f_{\rm beam}$ is the beam filling factor, $T_{\rm ex}$ is the excitation temperature of the transition (the line source function), $T_{\rm bg}$ represents a background radiation field, which at mm-wavelengths is the cosmic microwave radiation ($T_{\rm bg} = 2.725$ K), and τ is the line optical depth.

Assuming that the lines of $C^{34}S$ are formed in the same layers as the corresponding CS lines (= $C^{32}S$) and that the line opacities scale as their relative abundances, i.e. $x = \tau(C^{32}S)/\tau(C^{34}S) = X(^{32}S)/X(^{34}S)\,(= 22.5)$, means that the radiative transfer equation for the ratio of these lines reduces to $\frac{1-e^{-x\,\tau(34)}}{1-e^{-\tau(34)}} \approx \frac{T_{\rm mb}(\rm CS)_{(J,J-1)}}{T_{\rm mb}(C^{34}S)_{(J,J-1)}}$. This transcendental equation can be solved iteratively for the optical depth in the $C^{34}S$ lines, $\tau(34)$, and these are presented for a number of cores in Table 3. Quite in accordance with expectation, these values are all smaller than unity.

For the optically thin $C^{34}S$ lines we derive the excitation temperature and column density of the molecule from degenerated rotation diagrams (see, e.g., Goldsmith & Langer 1999). For these two transitions, i.e. the $C^{34}S$ (2-1) and (3-2) lines, the excitation temperatures, $T_{\rm ex}$, and column densities, $N(C^{34}S)$, are listed in Table 3. Having determined the opacities from the $C^{34}S$ lines, the same analysis can be done for the CS lines, which results in the values presented in Table 4 [4]. From this it is evident that the limited number of cores with detectable $C^{34}S$ emission has only moderately high optical depths in the lines of the main isotope of sulfur. The majority of cores can be expected therefore to exhibit $\tau \lesssim 1$.

From Tables 3 and 4 it is evident that the derived excitation temperatures are remarkably low. If these were meant to represent true gas kinetic temperatures, we have to conclude that assuming LTE (Local Thermodynamic Equilibrium) would likely be erroneous. Else, for unit beam filling, it would seem that the volume densities of cores, averaged over the beam, are generally lower than the critical densities of the transitions.

4.2. CS column densities and core masses

For the present sample, the analysis of the previous section, including maps of two transitions and of their weak isotopic lines, could be done only for a limited number of cores. The size of the analysable sample can be increased by applying the $C^{34}S$ method to the set of CS data for which two transitions have been observed. Assuming optically thin emission in the (2-1) and (3-2) lines of the main isotope (justified shortly), results in the $T_{\rm ex}$ distribution shown in Fig. 6 for 90 cores ($T_{\rm ex} > 3\sigma$). These temperatures are, again, generally quite low, 6 K on the average. For 69 cores ($N > 3\sigma$), the data quality permits the determination of the CS column densities, which are of the order of 10^{13} cm^{-2} and thus consistent with the values of Table 4.

These column densities are not extremely sensitive to the actual excitation temperature (within reasonable limits, of course), so that the adoption of a reasonable average value would permit us to use the entire data set. Consequently, we used (somewhat arbitrarily) the value of 10 K (see, e.g., 1). However, as will be demonstrated a posteriori, this choice is not critical to our final results (see below). Once $T_{\rm ex}$ is known, the line optical depth τ can be determined from the observations. This is shown in Fig. 7, where the distributions of both the CS (2-1) (291 cores) and (3-2) (131 cores) line depths are depicted. As expected, the optical depth in the (3-2) transition is larger than that in the (2-1) line. Also evident from the figure is the fact that the majority of cores is optically thin in these lines.

[4] Core IDs and coordinates are given in Table 6

Table 3. Excitation temperatures and column densities from $C^{34}S$ (2-1) and (3-2) observations

Core	$C^{34}S$ (2–1) T_{mb} (K)	ΔT (K)	$\int T_{mb}\,dv$ (K km s^{-1})	τ_{21}	$C^{34}S$ (3–2) T_{mb} (K)	ΔT (K)	$\int T_{mb}\,dv$ (K km s^{-1})	τ_{32}	T_{ex} (K)	$N(C^{34}S)$ (cm^{-2})
40	0.32	0.04	0.36	0.14	0.19	0.03	0.09	0.15	3.7	9.4×10^{12}
41	0.11	0.03	0.17	0.07		0.02		<0.10		
52	0.21	0.04	0.29	0.14	0.12	0.02		0.08		
58	0.14	0.03	0.03	0.17		0.02		<0.15		
60	0.13	0.03	0.06	0.09		0.02		<0.12		
61	0.15	0.03	0.09	0.12		0.02		<0.10		
64	0.13	0.03	0.15	0.09	0.08	0.02	0.04	0.16	4.0	3.3×10^{12}
65	0.12	0.03	0.08	0.08	0.09	0.02	0.08	0.16	12.6	6.7×10^{11}
66	0.14	0.03	0.14	0.08		0.02		<0.08		
74	0.21	0.03	0.10	0.16	0.09	0.02	0.06	0.04	7.6	8.4×10^{11}
76	0.21	0.04	0.15	0.10	0.08	0.02	0.07	0.03	5.8	1.6×10^{12}
82		0.04		<0.22		0.02		<0.30		
88	0.21	0.03	0.09	0.17	0.09	0.02	0.04	0.13	5.8	9.8×10^{11}
90	0.15	0.04	0.13	0.02	0.13	0.03	0.04	0.09	4.5	2.0×10^{12}
92	0.19	0.02	0.16	0.12		0.01		<0.03		
100	0.16	0.04	0.08	0.18		0.03		<0.14		
102		0.03		<0.15		0.02		<0.15		
106	0.09	0.03	0.08	0.13	0.10	0.02	0.05	0.29	7.1	7.4×10^{11}
115		0.02		<0.04		0.01		<0.10		
117	0.13	0.03	0.11	0.09	0.08	0.02	0.06	0.14	6.9	9.7×10^{11}
132	0.14	0.06	0.21	<0.13		0.04		<0.14		

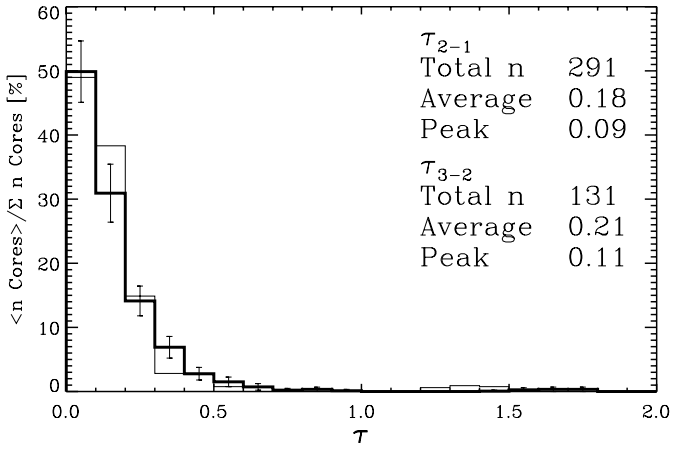

Fig. 7. Distribution of the line optical depth τ in the CS (2-1) transition (thick line) for a total of 291 cores and in the CS (3-2) transition (thin line) under the assumption of a uniform excitation temperature of 10 K (see the text).

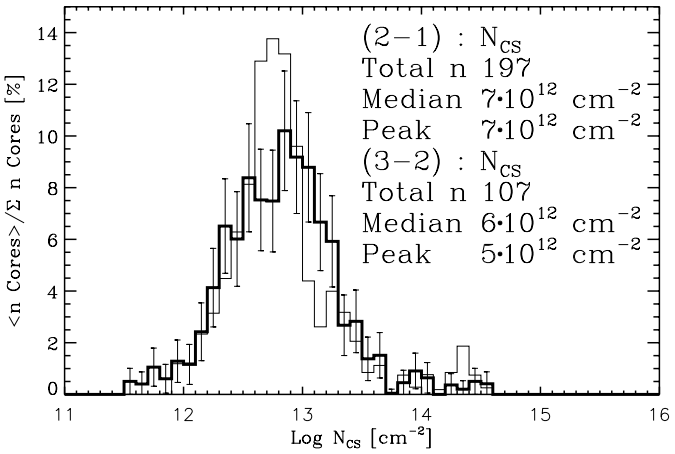

Fig. 8. CS column densities for T_{kin} = 10 K derived from the CS (2-1) (thick line) and CS (3-2) (thin line) transitions. These data are consistent with $N(CS) = 7 \times 10^{12}$ cm^{-2} for the majority of cores.

From these optically thin transitions we derive the CS column densities. These are shown in Fig. 8, separately for the CS (2-1) and (3-2) observations. Obviously, these distributions are very similar, the (2-1) data being less noisy. Both yield practically identical results, i.e. the median CS column density of nearly 200 cores is $N(CS) = 7 \times 10^{12}$ cm^{-2}. This is comparable with the values of Table 4 which were based on a more detailed and accurate analysis of the strong line cores.

Assuming a 'universal' CS abundance relative to H_2 of $X(CS) = 10^{-8}$ and a common distance of 500 pc, the column density distribution of Fig. 8 can be transformed into a core mass distribution (Fig. 9). As before (Sect. 4.3), this procedure is based on (for the area) adding the pixels with valid data ($> 3\sigma$) above the 50% peak value. For the sample of nearly 200 cores, the observed apparent mass range is from $10^{-2}\,M_\odot$ to $10^2\,M_\odot$, where the low mass cut-off is set by the lack of observational sensitivity. The median mass is 1 $M_\odot$, indicating that perhaps up to about 10^2 cores are Jeans-unstable.

The corresponding distribution of volume densities $n(H_2)$ can be obtained assuming that the extent of the core along the line of sight is similar to that in the plane of the sky, i.e. $n \approx N/\sqrt{\pi \times \text{area}}$ (Fig. 10). We find that the median density is $n(H_2) = 10^3$ cm^{-3}, at which the observed median line width (FWHM = 0.7 km s^{-1}) would correspond to a magnetic field strength of $B = 16\,\mu$G, if the CS lines were dominated by magnetic broadening. The corresponding critical mass would be $M_{crit} = 1.25\,(B/15\,\mu\text{G})\,(R/0.1\,\text{pc})^2\,M_\odot$ (Mouschovias & Spitzer

Table 4. Same as in Table 3, but for the corresponding $C^{32}S$ (2-1) and (3-2) observations

	CS (2–1)				CS (3–2)					
Core	T_{mb} (K)	ΔT (K)	$\int T_{mb}\,dv$ (K km s^{-1})	τ_{21}	T_{mb} (K)	ΔT (K)	$\int T_{mb}\,dv$ (K km s^{-1})	τ_{32}	T_{ex} (K)	N(CS) (cm^{-2})
40	2.33	0.08	1.78	3.23	1.27	0.07	1.04	3.43	6.9	1.6×10^{13}
41	1.31	0.05	1.37	1.58	0.62	0.06	0.67	<2.32	5.9	1.4×10^{13}
52	1.62	0.05	3.92	3.04	1.30	0.12	3.00	1.71	9.5	3.1×10^{13}
58	0.85	0.07	0.94	3.88	0.45	0.08	0.69	<3.37	9.0	7.6×10^{12}
60	1.28	0.05	1.10	2.10	0.57	0.08	0.44	<2.60	5.1	1.4×10^{13}
61	1.27	0.05	1.33	2.61	0.62	0.05	0.71	<2.35	6.5	1.3×10^{13}
64	1.27	0.06	2.09	2.05	0.57	0.06	0.77	3.52	4.8	2.9×10^{13}
65	1.34	0.06	1.51	1.70	0.60	0.07	0.55	3.59	4.7	2.1×10^{13}
66	1.47	0.06	1.53	1.84	0.60	0.06	0.70	<1.87	5.6	1.7×10^{13}
74	1.38	0.10	0.93	3.56	1.42	0.12	0.65	0.84	8.4	7.6×10^{12}
76	1.95	0.06	1.92	2.24	1.27	0.06	1.26	0.69	7.9	1.6×10^{13}
82	0.55	0.07	0.69	<4.85	0.27	0.08	0.32	<6.68	5.6	7.6×10^{12}
88	1.28	0.11	1.10	3.91	0.74	0.12	0.52	2.91	5.8	1.2×10^{13}
90	2.60	0.06	2.64	0.52	1.30	0.07	1.50	2.04	6.8	2.4×10^{13}
92	1.58	0.06	1.51	2.74	0.65	0.07	0.63	<0.72	5.2	1.8×10^{13}
100	0.92	0.10	0.31	4.06	0.60	0.13	0.18	<3.10	6.8	2.9×10^{12}
102	0.56	0.07	0.48	<3.45	0.37	0.09	0.18	<3.43	4.9	6.4×10^{12}
106	0.70	0.07	0.98	2.95	0.41	0.09	0.37	6.62	4.8	1.3×10^{13}
115	0.70	0.09	0.80	<0.94	0.41	0.11	0.22	<2.20	4.0	1.6×10^{13}
117	1.32	0.07	1.39	2.11	0.58	0.08	0.63	3.19	5.6	1.5×10^{13}
132	1.40	0.11	2.08	<2.96	0.90	0.11	0.52	<3.05	3.8	5.1×10^{13}

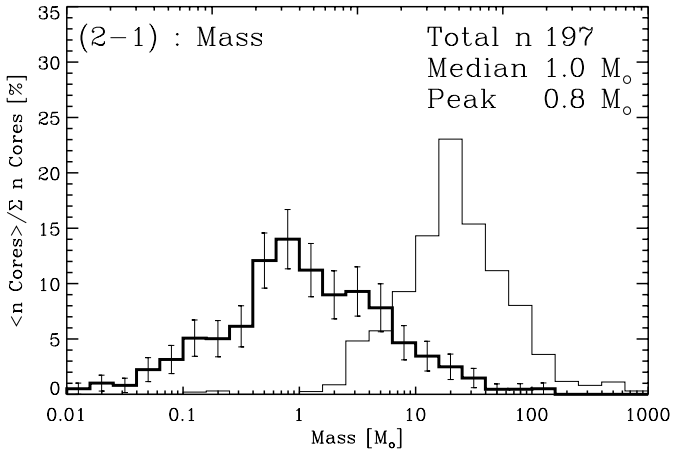

Fig. 9. The mass distribution for 197 cores from CS (2-1) observations is shown by the thick line. The assumptions include T_{kin} = 10 K, X(CS) = 10^{-8} and d = 500 pc yielding the median mass of 1 $M_\odot$. The light-line histogram shows the 'virial' mass of these cores, based on their observed line widths.

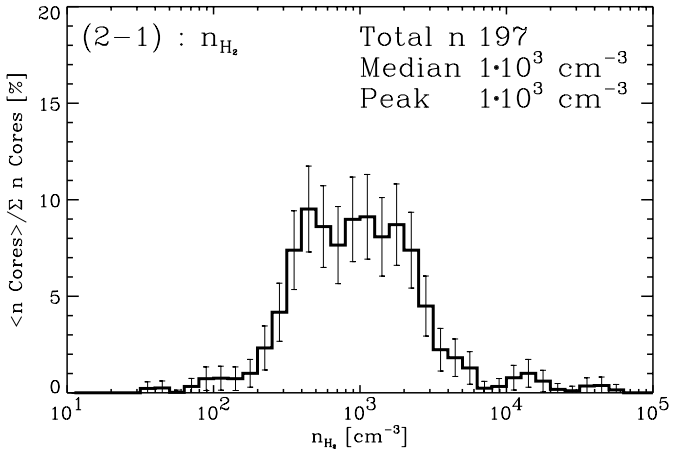

Fig. 10. Volume density distribution $n(H_2)$ for 197 cores from CS (2-1) observations (same assumptions as in caption of Fig. 9).

1976). The results of Fig. 9 could then suggest that less than half of the cores are potentially unstable.

However, from the results shown in Fig. 10, it is also evident that the (averaged) densities are much lower than the critical density of the CS (2-1) transition. This is clearly inconsistent with the assumption of LTE, since thermalisation of the level populations requires densities at least one order of magnitude above n_{crit}.

The actual value of the CS abundance could be lower than that assumed above. This is also suggested by the large relative offset of the virial mass distribution shown in Fig. 9, which is based on the observed line widths of the CS (2-1) line and the common distance of 500 pc. In fact, large variations for different locations in the Galaxy are indicated in the tabulation by Irvine et al. (1987). In particular, for the two well studied dark clouds TMC 1 and L 134N, X(CS) differs by one order of magnitude, with 10^{-9} in L 134N, possibly due to chemical evolution (Ohishi et al. 1992). If evolutionary effects are important for CS, then the application of a single abundance value to an ensemble of sources would of course be meaningless. On the other hand, this would open up the opportunity to use CS (in combination with other species) as a chemical clock.

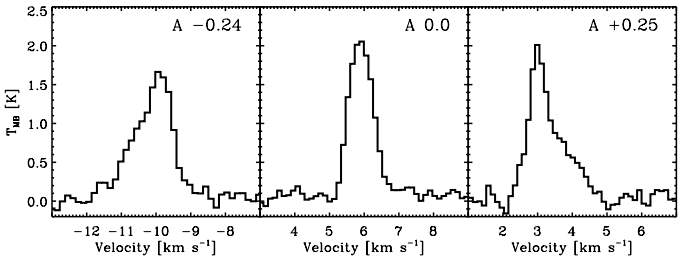

Fig. 11. Three types of observed CS (2-1) line profiles: blue-asymmetric (left), symmetric (centre) and red-asymmetric (right). Numerical values of the asymmetry parameter A are given in the right upper corner of each panel.

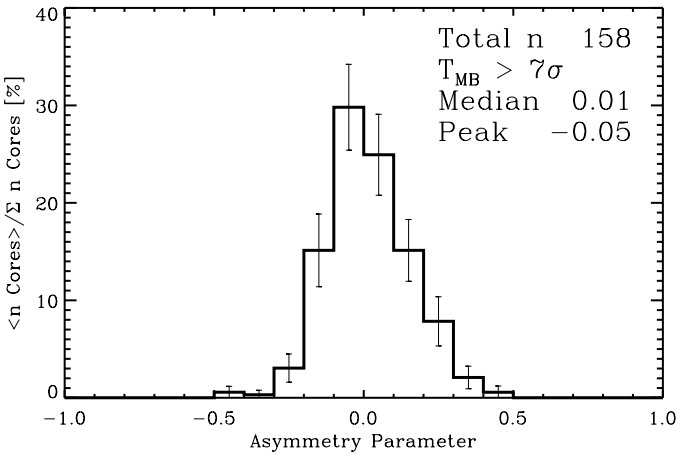

Fig. 12. The distribution of the asymmetry parameter A observed toward 158 cores in the CS(2-1) line. For 17% (27 cores) $A < -0.1$ and for 24% (38 cores) $A > 0.1$.

4.3. Line profiles

In order to avoid spurious effects due to the noise in the observed spectra we selected those observations the line intensity of which is above the 7σ level of the rms-noise (this particular value $T_{\rm mb,0} > 7\sigma$ was found empirically). Ideally, the velocity of the object with respect to the telescope υ_0 should be determined from optically thin lines, that are known to be symmetric. However, since we have only a limited amount of $C^{34}S$ data, the central (= systemic) velocities of the CS (2-1) lines were determined through the application of the high order moment $\upsilon\, T_{\rm mb}^3$ (to damp out the noise), i.e. $\upsilon_0 = \frac{\sum \upsilon\, T_{\rm mb}^3}{\sum T_{\rm mb}^3}$.

We then define an asymmetry parameter A as the difference between the integrated intensity on the positive side and on the negative side of the line centre υ_0, viz. $A = \frac{\int_{\upsilon_0}^{\infty} T_{\rm mb}\, d\upsilon - \int_{-\infty}^{\upsilon_0} T_{\rm mb}\, d\upsilon}{\int_{-\infty}^{\infty} T_{\rm mb}\, d\upsilon}$ and $|A| \in [0, 1]$. Examples of observed line asymmetries are shown in Fig. 11.

The result for those 158 cores for which $T_{\rm mb,0} > 7\sigma$ is shown in Fig. 12 (obtained toward the position of maximum CS (2-1) emission). Only 3% (5 cores) have a clear blue-asymmetry, with the asymmetry parameter $A < -0.2$, while a somewhat larger proportion, i.e. 11% (17 cores), are clearly red-asymmetric with $A > 0.2$. Evidently, the majority of cores reveals symmetric line profiles, with 41% (65 cores) displaying $|A| \in [-0.1, 0.1]$, perhaps indicating that outflows are not easily detectable in the lines of CS or have not yet developed in the cores.

5. Conclusions

Based on extensive mm-wave observations of a large sample of small dark cores in both celestial hemispheres in rotational lines of the CS molecule we conclude the following:

- The rate of CS detections is high. Specifically, out of 471 cores observed in CS (2-1), 315 were detected above 3σ. For CS (3-2), these numbers are 431 and 141, respectively.
- For 38% of the detected cores does the optical centre coincide with the position of maximum CS emission.
- Core temperatures are found to be low ($\lesssim$10 K).
- On the scales of these observations, the majority of cores is optically thin in the CS emission, with the median column density $N(\mathrm{CS}) = 7 \times 10^{12}\,\mathrm{cm}^{-2}$.
- The lines are generally symmetric and narrow, but wider than due to thermal broadening alone. The median line width is $\mathrm{FWHM} = 0.7\,\mathrm{km\,s}^{-1}$.

Acknowledgements. We thank the referee, Dr. Jan Brand, for his valuable comments on the manuscript. Special thanks go also to S. Nasoudi-Shoar and F. Saunier for their contributions to the project. This work was supported by the Swedish Science Research Council (NFR) and the Swedish National Space Board (SNSB).

References

[1] Benson P.J. & Mayers P.C., 1989, ApJS, 71, 89
[2] Bohlin R.C., Savage B.D. & Drake J.F., 1978, ApJ 224, 132
[3] Chandra, S., Kegel, W. H., Le, R. R. J., & Hertenstein, T. 1995, VizieR Online Data Catalog, 411
[4] Ciolek, G. E. & Mouschovias, T. C. 1995, ApJ, 454, 194
[5] Clemens D.P. & Barvainis R., 1988, ApJS, 68, 27
[6] Dame, T. M., Ungerechts, H., Cohen, R. S., et al. 1987, ApJ, 322, 706
[7] Feitzinger, J. V. & Stüwe, J. A. 1985, Bulletin d'Information du Centre de Donnees Stellaires, 28, 161
[8] Goldsmith P.F. & Langer W.D., 1987, ApJ, 222, 881
[9] Goldsmith P.F. & Langer W.D., 1999, ApJ, 517, 209
[10] Hartley M., Manchester R.M., Smith R.M., et al., 1986, A&AS, 63, 27
[11] Herbst W.& Sawyer D.L., 1981, ApJ 243, 935
[12] Irvine W.M., Goldsmith P.F. & Hjalmarson A., 1987, in: Hollenbach D. & Thronson H. (eds.), Interstellar processes, Dordrecht, D. Reidel Publishing, p. 561
[13] Jeans J.H., 1927, MNRAS, 87, 720
[14] Larsson, B., Liseau, R. & Men'shchikov, A. B., et al. 2000, A&A, 363, 253
[15] Loren R.B., Wootten A. & Wilking B.A.,1990, ApJ, 365, 269
[16] Mouschovias, T. C. & Spitzer, Jr., L. 1976, ApJ, 210, 326
[17] Ohishi, M., Irvine, W. M., & Kaifu, N. 1992, in IAU Symposium, Vol. 150, Astrochemistry of Cosmic Phenomena, ed. P. D. Singh, 171
[18] Pineiro, A. L., Tipping, R. H., & Chackerian, Jr., C. 1987, Journal of Molecular Spectroscopy, 125, 91
[19] Sandqvist A., 1977, A&A 57, 467S
[20] Sugitani K., Fukai Y. & Ogura K., 1991, ApJS, 77, 59
[21] Turner B.E., Kin-Wing C., Green S. & Lubowich D.A., 1992, ApJ, 399, 114
[22] Zealey W.J., Ninkov Z., Rice E., Hartley M. & Tritton S.B., 1983, ApL 23, 119

Table 5. CS (2-1) and (3-2) observations of cores (for a description, see the end of the table).

	Nr	α (2000)	2−1	v	τ_{2-1}		Nr	α (2000)	2−1	v	τ_{2-1}		Nr	α (2000)	2−1	v	τ_{2-1}
	Obs	δ (2000)	3−2	Δv	log N		Obs	δ (2000)	3−2	Δv	log N		Obs	δ (2000)	3−2	Δv	log N
	1	0 3 58.7	2.2	−10.0	0.3		28	3 56 36.5	0.3	2.3	0.1		55	7 17 33.9	(0.08)		
	OK	68 34 41	1.5	1.3	13.3		OK	56 8 2	(0.10)	0.5			SS	−23 1 35	(0.10)		
	2	0 5 24.4	2.8	−11.3	0.2		29	4 3 18.3	(0.12)				56	7 18 2.2	(0.09)		
	OK	67 17 39	1.7	1.8	13.4		OK	56 50 8	(0.11)				SS	−23 35 6	(0.11)		
	3	0 14 41.7	(0.15)				30	4 4 37.9	0.9	−4.7	0.2		57	7 18 13.1	0.1	4.9	0.0
	O	64 9 40					OK	56 56 11	0.4	0.6	12.9		SS	−23 38 52	(0.09)	0.5	
	4	0 19 4.2	0.6	−2.4	0.1		31	4 5 0.5	1.0	−2.9	0.2		58	7 18 15.1	0.9	14.9	0.1
	OK	63 55 31	(0.12)	0.8	12.7		OK	60 32 19	0.3	0.7	12.9		SS	−23 41 42	0.7	1.0	12.9
	5	0 28 45.7	0.7	−38.4	0.1		32	4 4 47.5	1.2	6.7	0.3		59	7 19 31.1	(0.24)		
	O	56 42 8		0.9			O	26 19 42		0.7	13.1		O	3 56 51			
	6	0 39 3.0	0.2	−11.4	0.1		33	4 25 10.5	(0.12)				60	7 29 32.7	1.0	−1.2	0.2
	OK	52 51 29	(0.10)	0.2			OK	54 19 11	(0.11)				SS	−41 10 30	0.5	0.6	12.9
	7	0 44 6.3	(0.19)				34	4 30 52.0	0.9	3.1	0.3		61	7 40 47.3	1.3	−4.1	0.2
	OK	62 30 2	(0.12)				OK	54 51 55	0.4	0.6	12.9		SS	−41 26 57	0.7	0.9	13.1
	8	0 49 28.6	0.6	−12.4	0.2		35	4 58 29.6	0.4	4.5	0.1		62	7 40 51.7	0.7	−3.6	0.2
	OK	50 44 41	(0.12)	0.4	12.7		OK	52 15 41	(0.11)	0.6			SS	−43 49 10	0.8	0.6	12.8
	9	0 59 4.0	(0.13)				36	4 59 4.0	(0.12)				63	7 42 30.3	1.1	−3.9	0.1
	O	60 53 32					OK	52 3 24	(0.11)				SS	−42 5 10	0.4	1.1	13.0
	10	1 12 15.8	0.8	−0.3	0.1		37	5 0 9.2	0.5	5.8	0.1		64	7 42 48.7	2.1	−3.9	0.2
	OK	64 25 55	0.1	1.1	12.8		OK	52 4 60	(0.12)	0.5			SS	−42 25 47	0.8	1.5	13.3
	11	1 23 56.6	(0.17)				38	5 4 9.7	0.5	7.2	0.3		65	7 43 5.3	1.5	−5.2	0.2
	OK	74 22 31	(0.12)				O	32 43 9		0.4			SS	−42 7 30	0.5	1.0	13.1
	12	1 29 51.8	(0.12)				39	5 4 15.3	0.5	7.1	0.2		66	7 43 34.9	2.3	−4.6	0.3
	O	63 5 29					O	32 47 29		0.4	12.6		SS	−42 22 2	0.9	1.3	13.3
	13	1 30 50.1	0.3	−0.3	0.1		40	5 6 20.2	1.8	8.8	0.4		67	7 45 10.4	0.1	8.3	0.1
	OK	67 23 46	(0.12)	0.9			SS	−3 56 2	1.0	0.7	13.2		SS	−34 36 14	(0.10)	0.3	11.8
	14	1 37 2.3	0.7	−10.5	0.1		41	5 22 11.4	1.4	11.3	0.2		68	8 4 35.6	(0.09)		
	OK	65 2 43	(0.14)	1.1	12.8		SS	−3 41 34	0.7	1.0	13.1		SS	−31 30 47	(0.10)		
	15	1 38 37.3	1.6	−11.7	0.4		42	5 23 30.1	(0.13)				69	8 5 26.3	0.6	8.9	0.1
	OK	65 5 14	0.9	0.7	13.2		O	33 11 54					SS	−39 8 56	0.2	1.1	12.7
	16	1 56 54.6	0.4	−11.4	0.1		43	5 29 44.3	0.4	0.2			70	8 9 31.6	3.6	6.0	0.5
	OK	62 41 18	(0.11)	0.6	12.5		OK	5 45 3	(0.11)	0.2			SS	−36 4 47	2.2	1.1	
	17	1 57 35.9	0.2	−11.4	0.1		44	5 44 29.7	2.8	12.0	0.4		71	8 10 9.5	(0.13)		
	OK	62 39 37	(0.14)	0.4			OK	9 8 54	1.1	1.3	13.4		SS	−38 43 26	(0.10)		
	18	2 29 1.7	5.6	−51.4	0.5		45	5 46 36.9	(0.26)				72	8 12 21.0	0.4	5.4	0.1
	O	61 33 33		1.8	13.8		OK	20 45 31	(0.11)				SS	−33 56 15	(0.10)	0.6	12.5
	19	2 34 45.0	(0.14)				46	6 0 38.9	1.5	1.3	0.2		73	8 12 22.9	0.5	5.3	0.1
	O	60 47 48					OK	31 39 30	0.6	1.3	13.1		SS	−34 1 4	0.4	0.4	
	20	2 34 52.1	1.1	−39.7	0.2		47	6 0 56.0	0.3	3.1	0.1		74	8 12 25.3	0.9	5.0	0.2
	O	61 46 47		2.2	13.0		OK	16 56 50	(0.13)	0.5			SS	−33 45 40	0.6	0.6	
	21	2 35 37.4	(0.12)				48	6 3 11.6	0.4	3.5	0.2		75	8 12 22.6	1.0	9.4	0.2
	O	61 19 36					OK	16 37 6	(0.13)	0.5			SS	−38 50 4	0.6	0.7	13.0
	22	2 36 27.1	(0.12)				49	6 8 55.2	0.9	0.5	0.3		76	8 14 21.4	1.9	4.7	0.3
	O	61 23 37					OK	17 50 19	(0.12)	0.5	12.9		SS	−34 30 53	1.3	0.9	
	23	2 48 15.3	(0.12)				50	6 22 58.7	1.0	−5.1	0.1		77	8 14 35.5	0.9	8.2	0.1
	O	60 24 36					OK	23 9 58	(0.11)	1.4	12.9		SS	−42 5 12	0.5	0.9	
	24	2 51 28.9	1.2	−39.8	0.2		51	6 48 42.9	0.7	17.0	0.1		78	8 14 34.8	0.1	4.8	0.1
	O	60 3 14		1.0	13.0		SS	−16 53 27	0.2	1.2	12.7		SS	−44 5 54	(0.09)	0.6	
	25	2 55 2.9	3.8	−37.9	0.4		52	7 4 16.8	3.9	19.6	0.3		79	8 15 7.2	(0.10)		
	O	60 35 45		1.5	13.6		SS	−16 24 33	3.0	2.3			SS	−38 41 2	(0.05)		
	26	3 1 0.7	2.2	−38.6	0.3		53	7 4 44.6	(0.09)				80	8 15 28.2	0.4	1.6	0.1
	O	60 40 21		1.3	13.3		SS	−16 35 42	(0.10)				SS	−34 4 45	(0.11)	0.5	
	27	3 1 32.2	12.3	−38.0	1.0		54	7 14 36.0	(0.08)				81	8 15 59.5	1.2	2.0	0.4
	O	60 29 12		2.5	14.2		SS	−25 8 54	(0.10)				SS	−33 50 47	0.9	0.6	13.1

Table 5. Continued

	Nr	α (2000)	2−1	v	τ_{2-1}	Nr	α (2000)	2−1	v	τ_{2-1}	Nr	α (2000)	2−1	v	τ_{2-1}
	Obs	δ	3−2	Δv	log N	Obs	δ	3−2	Δv	log N	Obs	δ	3−2	Δv	log N
	82	8 16 37.7	0.5	9.7	0.1	109	9 15 32.2	0.3	3.6	0.0	136	11 32 2.2	(0.10)		
	SS	−42 7 55	(0.08)	0.8	12.6	SS	−41 13 32	0.1	1.2	12.3	SS	−64 23 16	(0.12)		
	83	8 16 35.6	0.1	6.1	0.0	110	9 16 9.1	(0.09)			137	11 33 51.9	(0.13)		
	SS	−52 54 32	(0.11)	0.5	12.0	SS	−41 18 58	(0.12)			0	79 30 39			
	84	8 17 10.6	1.1	8.6	0.2	111	9 18 47.4	0.5	1.4	0.1	138	11 34 44.6	(0.10)		
	SS	−39 52 57	0.6	0.8	13.0	SS	−44 19 12	0.2	0.7	12.6	SS	−64 34 41	(0.13)		
	85	8 17 12.2	0.4	5.5	0.1	112	9 25 44.7	(0.10)			139	11 37 33.0	0.0	5.5	0.0
	SS	−52 43 22	(0.10)	0.7	12.5	SS	−48 23 37	(0.11)			SS	−61 44 37	(0.12)	1.0	
	86	8 18 39.9	0.3	2.7	0.1	113	9 26 7.1	0.3	−2.3	0.1	140	11 42 50.8	(0.10)		
	SS	−49 43 51	(0.08)	0.8	12.4	SS	−48 15 2	(0.11)	0.4	12.5	SS	−61 44 21	(0.12)		
	87	8 19 15.7	(0.10)			114	9 27 14.3	(0.09)			141	11 43 31.1	(0.10)		
	SS	−42 54 47	(0.08)			SS	−48 16 47	(0.11)			SS	−59 2 33	(0.12)		
	88	8 20 33.4	1.1	3.6	0.2	115	9 27 34.0	0.8	−1.7	0.1	142	11 48 0.7	(0.10)		
	SS	−50 5 34	0.5	0.8	13.0	SS	−48 32 54	0.2	1.0	12.8	SS	−61 26 4	(0.13)		
	89	8 21 20.9	0.3	5.4	0.0	116	9 28 21.2	0.0	−2.8	0.0	143	11 48 9.7	(0.12)		
	SS	−52 26 25	(0.12)	0.9	12.4	SS	−48 33 14	(0.11)	0.4		SS	−61 30 34	(0.14)		
	90	8 25 44.3	2.6	5.2	0.5	117	9 28 47.0	1.4	5.8	0.2	144	11 51 28.6	0.4	−12.6	0.1
	SS	−51 2 5	1.5	0.9	13.4	SS	−51 36 39	0.6	1.0	13.1	SS	−61 2 53	(0.14)	0.7	
	91	8 26 11.9	0.4	6.1	0.1	118	9 29 7.4	0.6	−4.2	0.1	145	12 3 57.0	(0.11)		
	SS	−51 39 18	(0.08)	1.0	12.5	SS	−48 32 34	(0.11)	1.8	12.7	SS	−60 1 54	(0.14)		
	92	8 26 34.3	1.5	4.8	0.3	119	9 31 2.7	0.8	−4.8	0.1	146	12 6 16.2	0.1	−16.3	0.1
	SS	−50 39 55	1.0	0.7	13.1	SS	−48 38 21	(0.11)	0.9	12.8	SS	−60 9 12	(0.14)	0.5	
	93	8 26 39.5	1.8	5.9	0.3	120	9 36 43.9	0.3	−5.1	0.1	147	12 7 8.4	0.2	−4.4	0.1
	SS	−51 1 38	0.7	0.9	13.2	SS	−48 51 54	0.1	0.5	12.3	SS	−65 18 42	(0.12)	0.8	
	94	8 32 0.8	0.6	5.6	0.1	121	9 38 53.2	(0.10)			148	12 22 8.5	0.2	−5.8	0.1
	SS	−50 32 50	(0.14)	0.7	12.7	SS	−51 28 42	(0.12)			SS	−66 27 8	0.1	0.5	
	95	8 32 42.5	(0.11)			122	9 45 1.1	0.4	−5.2	0.1	149	12 32 27.3	0.6	3.5	0.1
	SS	−39 25 4	(0.13)			SS	−48 51 21	0.1	0.8	12.5	SS	−70 45 15	(0.14)	0.7	
	96	8 36 54.1	(0.11)			123	9 45 26.5	0.8	−6.4	0.1	150	12 34 21.4	(0.11)		
	SS	−48 3 31	(0.14)			SS	−50 38 34	(0.13)	1.8	12.8	SS	−70 28 50	(0.14)		
	97	8 37 18.3	0.4	10.4	0.1	124	9 45 52.2	0.1	11.0	0.1	151	12 36 18.6	0.6	−4.9	0.2
	SS	−36 37 56	(0.12)	0.1	12.5	SS	−48 18 11	(0.12)	0.9		SS	−63 12 36	0.3	0.5	
	98	8 44 13.9	0.3	2.0	0.1	125	10 25 27.2	(0.09)			152	12 37 8.9	0.0	4.0	0.1
	SS	−59 54 2	(0.12)	0.6	12.3	SS	−59 25 10	(0.10)			SS	−69 59 54	(0.11)	0.3	
	99	8 52 38.2	0.5	2.0	0.1	126	10 36 0.1	(0.09)			153	12 39 39.8	0.3	−5.2	0.1
	SS	−50 40 5	(0.13)	0.6		SS	−61 7 34	(0.11)			SS	−65 26 28	(0.11)	0.5	12.3
	100	8 52 35.6	0.3	3.6	0.1	127	10 38 12.7	0.9	−13.4	0.1	154	12 41 1.5	0.5	1.1	0.1
	SS	−51 51 53	0.2	0.5		SS	−60 11 43	0.3	1.7	12.9	SS	−80 19 45	(0.12)	1.0	12.6
	101	8 53 15.1	(0.10)			128	10 43 22.1	0.8	−26.1	0.1	155	12 40 54.6	(0.09)		
	SS	−41 52 24	(0.13)			SS	−60 15 3	(0.11)	2.3	12.8	SS	−69 52 15	(0.08)		
	102	8 53 25.0	0.5	5.4	0.1	129	10 48 59.5	0.8	−8.0	0.1	156	12 47 50.8	(0.09)		
	SS	−41 57 19	0.2	0.7	12.6	SS	−62 23 5	(0.11)	1.6	12.8	SS	−69 14 52	(0.11)		
	103	8 53 42.5	0.0	6.5	0.1	130	11 4 43.6	0.6	−24.7	0.1	157	12 48 46.0	0.3	1.2	0.1
	SS	−44 48 2	(0.12)	0.5		SS	−58 10 60	(0.10)	0.9	12.7	SS	−79 39 21	0.0	0.7	12.4
	104	8 56 37.5	0.4	6.1	0.0	131	11 14 28.6	2.0	−6.1	0.2	158	12 50 24.4	0.1	1.7	0.1
	SS	−46 51 35	(0.12)	1.3	12.5	SS	−60 53 3	1.2	1.6	13.2	SS	−79 38 14	(0.12)	0.6	12.0
	105	8 57 27.5	(0.09)			132	11 27 51.5	2.1	−27.6	0.2	159	12 58 54.8	−0.0	−1.1	0.0
	SS	−46 58 20	(0.12)			SS	−62 9 55	0.5	1.5	13.3	SS	−61 20 17	(0.11)	0.8	
	106	8 57 34.1	1.0	6.0	0.1	133	11 29 33.4	(0.10)			160	13 3 14.7	0.6	3.4	0.2
	SS	−46 40 44	0.4	1.4	12.9	SS	−60 42 27	(0.11)			SS	−77 23 0	0.3	0.5	12.7
	107	9 13 24.7	(0.03)			134	11 29 56.4	0.3	−7.9	0.1	161	13 5 24.3	0.4	3.5	0.1
	SS	−40 29 32	(0.12)			SS	−60 58 15	(0.11)	0.7	12.3	SS	−77 40 46	(0.14)	0.5	
	108	9 13 50.0	0.2	9.4	0.1	135	11 30 10.4	(0.11)			162	13 5 53.3	0.2	2.1	0.0
	SS	−40 21 39	(0.12)	0.6	12.3	SS	−61 13 21	(0.12)			SS	−77 52 45	(0.14)	0.7	

Table 5. Continued

	Nr	α (2000)	2−1	v	τ_{2-1}		Nr	α (2000)	2−1	v	τ_{2-1}		Nr	α (2000)	2−1	v	τ_{2-1}
	Obs	δ	3−2	Δv	log N		Obs	δ	3−2	Δv	log N		Obs	δ	3−2	Δv	log N
	163	13 6 30.3	0.4	3.6	0.1		190	15 45 35.9	0.4	5.0	0.1		217	16 27 37.2	(0.11)		
	SS	−78 2 21	(0.15)	0.4			SS	−34 38 56	(0.16)	1.0	12.5		SS	−24 42 28	(0.14)		
	164	13 19 31.3	1.0	−32.6	0.1		191	15 50 16.6	0.4	−9.5	0.1		218	16 28 29.1	2.0	3.7	0.5
	SS	−62 33 27	(0.14)	1.8	12.9		SS	−45 30 28	(0.11)	0.7			SS	−24 18 25	1.1	0.6	13.3
	165	13 24 32.3	(0.09)				192	15 50 48.6	0.3	2.9	0.1		219	16 28 31.4	(0.08)		
	SS	−57 17 1	(0.13)				SS	−4 6 14	(0.12)	0.8			SS	−24 19 7	(0.21)		
	166	13 25 48.6	0.8	−33.1	0.1		193	15 53 36.3	0.7	2.9	0.1		220	16 30 3.7	0.4	4.1	0.1
	SS	−59 42 53	0.0	1.2	12.8		SS	−4 35 26	0.8	0.6			SS	−39 9 0	(0.16)	0.4	12.5
	167	13 28 52.0	1.5	−28.6	0.3		194	15 54 12.1	0.6	2.6	0.1		221	16 31 18.7	0.3	2.8	0.1
	SS	−62 27 30	−0.1	0.9	13.1		SS	−2 49 42	0.3	0.6			SS	−23 41 21	(0.14)	0.4	
	168	13 30 2.8	(0.13)				195	16 1 8.3	0.8	−16.3	0.2		222	16 31 35.6	1.9	2.9	0.3
	0	79 22 34					SS	−53 46 30	(0.13)	0.8	12.8		SS	−24 1 27	0.5	0.8	13.2
	169	14 13 18.7	0.2	−2.9	0.1		196	16 0 10.1	(0.12)				223	16 32 2.3	2.8	4.7	0.4
	SS	−57 37 43	(0.13)	0.4			SS	−1 26 44	(0.13)				SS	−24 56 11	0.9	1.1	13.4
	170	14 26 57.9	0.1	−3.0	0.0		197	16 2 49.2	0.2	4.2	0.1		224	16 32 22.7	9.4	4.1	0.6
	SS	−55 27 34	(0.10)	0.4			SS	−42 13 41	(0.12)	0.8			SS	−24 28 33	16.0	2.8	14.0
	171	14 53 21.3	0.0	−7.6			198	16 3 15.0	0.4	3.8	0.1		225	16 32 42.0	1.5	2.8	0.3
	SS	−61 36 3	(0.11)	0.5			SS	−42 6 27	(0.12)	0.8	12.6		SS	−23 54 9	1.2	0.9	13.1
	172	14 56 35.1	0.3	25.7	0.1		199	16 4 28.8	0.4	4.4	0.1		226	16 33 26.6	1.3	2.2	0.2
	SS	−56 29 47	(0.14)	0.6			SS	−39 37 46	(0.13)	0.5	12.5		SS	−36 36 34	0.6	1.0	13.0
	173	15 0 19.6	0.2	−17.1	0.1		200	16 9 17.3	0.2	5.2	0.1		227	16 34 33.2	3.0	0.7	0.4
	SS	−56 59 35	(0.16)	0.4			SS	−41 49 58	(0.11)	0.5			SS	−15 47 11	2.4	1.0	13.5
	174	15 2 56.2	(0.10)				201	16 10 41.6	0.9	9.5	0.1		228	16 34 37.5	2.5	1.0	0.4
	SS	−63 42 34	(0.14)				SS	−37 52 22	0.5	1.1	12.9		SS	−15 47 1	1.2	0.7	13.4
	175	15 3 37.1	0.0	−21.8	0.1		202	16 12 43.2	1.3	−5.3	0.2		229	16 36 40.1	0.4	−2.8	0.1
	SS	−64 31 50	(0.14)	0.4			SS	−52 15 34	1.1	1.2	13.0		SS	−46 1 16	(0.04)	0.6	
	176	15 5 12.0	0.0	−6.5	0.1		203	16 18 46.5	0.1	4.5	0.0		230	16 36 50.2	0.6	3.3	0.2
	SS	−64 7 57	(0.14)	0.5			SS	−36 42 39	(0.10)	0.3			SS	−35 37 8	(0.12)	0.5	
	177	15 11 13.4	(0.10)				204	16 20 4.4	(0.12)				231	16 36 51.8	0.1	3.8	0.1
	SS	−53 18 25	(0.13)				SS	−53 18 23	(0.13)				SS	−35 56 32	(0.12)	0.4	
	178	15 15 13.6	(0.11)				205	16 19 40.0	0.6	4.5	0.1		232	16 37 16.1	(0.12)		
	SS	−60 13 37	(0.14)				SS	−38 11 41	(0.13)	0.7	12.7		SS	−35 31 37	(0.13)		
	179	15 17 31.6	0.4	−8.8	0.1		206	16 22 37.2	0.1	4.2	0.1		233	16 37 27.6	0.8	3.8	0.2
	SS	−62 39 29	(0.14)	0.6			SS	−40 23 12	(0.13)	0.4			SS	−35 13 54	0.3	0.6	12.9
	180	15 17 12.8	0.6	−9.0	0.1		207	16 23 37.8	0.6	−20.6	0.2		234	16 37 46.0	0.3	3.2	0.1
	SS	−50 36 41	(0.17)	0.8			SS	−49 32 57	(0.04)	0.7	12.7		SS	−35 26 23	(0.13)	0.6	12.4
	181	15 21 1.8	−0.3	−11.1	0.1		208	16 26 5.1	0.8	4.6	0.2		235	16 38 52.7	0.3	3.4	0.1
	SS	−50 12 17	(0.12)	0.3			SS	−41 15 22	0.0	0.5	12.8		SS	−35 49 48	(0.13)	0.5	
	182	15 21 35.5	(0.10)				209	16 26 12.0	0.3	4.1	0.1		236	16 39 30.3	(0.10)		
	SS	−59 35 51	(0.13)				SS	−38 25 9	(0.16)	0.5			SS	−14 5 51	(0.13)		
	183	15 24 30.9	(0.11)				210	16 26 26.4	11.3	3.3	1.7		237	16 44 18.7	(0.10)		
	SS	−63 3 24	(0.14)				SS	−24 24 33	11.7	1.8	14.3		SS	−49 14 39	(0.13)		
	184	15 25 2.8	0.5	0.8	0.1		211	16 26 53.0	3.6	3.8	0.5		238	16 45 1.0	(0.09)		
	SS	−61 1 40	(0.14)	0.7			SS	−24 32 31	2.5	1.1	13.6		SS	−47 45 12	(0.12)		
	185	15 25 45.4	1.0	−0.6	0.1		212	16 27 1.9	3.4	4.2	0.2		239	16 44 50.3	0.2	4.6	0.1
	SS	−61 7 8	(0.13)	0.9	12.9		SS	−24 38 30	1.7	2.4	13.5		SS	−40 23 6	(0.13)	0.4	12.2
	186	15 26 26.8	(0.10)				213	16 27 10.4	6.1	3.4	0.9		240	16 46 45.1	(0.11)		
	SS	−61 55 59	(0.13)				SS	−24 29 30	4.2	1.4	13.9		SS	−46 27 22	(0.14)		
	187	15 26 17.5	(0.10)				214	16 27 19.1	3.4	3.0	0.6		241	16 46 44.8	0.4	5.2	0.1
	SS	−49 59 29	(0.15)				SS	−24 24 29	2.6	0.8	13.6		SS	−44 30 46	(0.12)	0.5	
	188	15 27 12.0	(0.11)				215	16 27 28.0	(0.12)				242	16 47 6.6	0.5	3.6	0.2
	SS	−62 23 15	(0.14)				SS	−24 26 29	(0.15)				SS	−9 35 21	0.2	0.5	12.7
	189	15 27 2.7	−0.1	−10.6	0.1		216	16 27 35.6	2.0	4.1	0.3		243	16 47 23.1	0.7	4.2	0.1
	SS	−50 0 38	(0.12)	0.8			SS	−24 43 26	1.2	1.0	13.3		SS	−13 59 21	(0.13)	0.9	12.8

Table 5. Continued

	Nr	α (2000)	2−1	v	τ_{2-1}		Nr	α (2000)	2−1	v	τ_{2-1}		Nr	α (2000)	2−1	v	τ_{2-1}
	Obs	δ	3−2	Δv	log N		Obs	δ	3−2	Δv	log N		Obs	δ	3−2	Δv	log N
	244	16 48 6.8	1.1	3.0	0.3		271	17 15 2.1	0.7	1.1	0.2		298	17 54 42.9	0.5	8.3	0.1
	SS	−10 51 48	0.4	0.6	13.0		SS	−20 29 60	(0.15)	0.6	12.8		SS	−27 49 56	(0.10)	0.6	
	245	16 48 8.5	1.3	3.2	0.4		272	17 15 30.2	(0.12)				299	17 55 6.4	(0.10)		
	SS	−10 56 58	1.1	0.6	13.1		SS	−32 24 56	(0.15)				SS	−32 37 5	(0.12)		
	246	16 49 9.4	(0.12)				273	17 15 14.6	(0.12)				300	17 55 12.2	(0.10)		
	SS	−39 45 6	(0.12)				SS	−1 43 20	(0.16)				SS	−34 15 40	(0.11)		
	247	16 50 15.4	1.2	6.0	0.2		274	17 19 35.8	0.9	−7.7	0.1		301	17 55 25.0	0.1	6.4	0.1
	SS	−18 6 6	0.6	0.9	13.0		SS	−43 27 3	0.1	1.0	12.9		SS	−2 48 45	(0.13)	0.4	
	248	16 50 33.7	0.6	4.6	0.2		275	17 19 43.7	0.6	3.5	0.1		302	17 55 31.4	(0.10)		
	SS	−19 7 50	0.0	0.6	12.7		SS	−26 43 2	(0.11)	0.9	12.7		SS	−8 15 26	(0.13)		
	249	16 54 32.3	1.4	−17.4	0.2		276	17 20 56.2	(0.13)				303	17 58 6.1	−0.0	7.0	0.1
	SS	−40 31 8	0.7	1.5	13.1		SS	−33 31 21	(0.15)				SS	−3 46 21	(0.12)	0.5	
	250	16 57 16.2	0.9	5.3	0.2		277	17 21 47.5	3.0	−13.3	0.3		304	18 1 9.8	0.0	−10.6	0.0
	SS	−16 9 22	(0.14)	0.6	12.9		SS	−44 8 48	2.5	1.6			SS	−32 49 44	(0.11)	0.9	
	251	16 58 41.8	(0.10)				278	17 21 50.0	0.1	2.6	0.0		305	18 0 34.8	(0.10)		
	SS	−50 35 45	(0.12)				SS	−21 48 24	(0.14)	1.1	12.0		SS	−3 30 36	(0.13)		
	252	16 58 25.5	(0.10)				279	17 22 37.3	0.5	4.0	0.2		306	18 1 17.0	(0.10)		
	SS	−36 42 15	(0.13)				SS	−27 5 1	0.4	0.5			SS	−32 58 14	(0.11)		
	253	17 2 20.0	0.5	17.1	0.1		280	17 22 36.8	0.4	3.6	0.1		307	18 3 2.5	0.7	5.7	0.1
	SS	−33 16 34	(0.14)	0.9			SS	−23 50 34	(0.15)	0.5			SS	−46 39 49	0.4	0.9	
	254	17 2 42.0	0.0	18.7	0.1		281	17 25 11.5	0.2	−36.4	0.0		308	18 2 58.0	0.5	11.3	0.1
	SS	−33 16 60	(0.13)	0.5	11.6		SS	−40 16 27	(0.12)	1.2	12.2		SS	−27 52 8	(0.11)	1.0	12.6
	255	17 3 0.1	0.4	2.8	0.1		282	17 30 37.7	0.2	−13.3	0.1		309	18 3 15.1	(0.10)		
	SS	−22 13 39	(0.05)	0.4			SS	−43 8 28	(0.12)	0.9	12.3		SS	−33 1 5	(0.12)		
	256	17 4 26.2	0.7	12.6	0.1		283	17 32 14.2	0.5	4.1	0.1		310	18 3 4.1	0.3	5.5	0.0
	SS	−36 18 50	(0.13)	0.9	12.8		SS	−25 25 29	(0.12)	0.7	12.6		SS	−20 51 0	(0.11)	1.0	12.4
	257	17 4 26.9	0.9	11.3	0.1		284	17 35 10.7	0.2	10.8	0.1		311	18 5 3.9	(0.10)		
	SS	−36 8 26	(0.14)	1.4	12.9		SS	−33 32 37	(0.12)	0.6	12.3		SS	−28 25 54	(0.11)		
	258	17 4 46.0	0.4	11.7	0.1		285	17 35 26.4	0.2	−5.9	0.1		312	18 5 55.9	(0.10)		
	SS	−36 10 18	0.3	0.6	12.5		SS	−33 21 36	(0.11)	1.0	12.3		SS	−18 25 13	(0.11)		
	259	17 4 48.8	0.3	11.2	0.1		286	17 38 26.5	0.3	10.8	0.1		313	18 7 13.8	0.7	6.8	0.1
	SS	−36 3 36	(0.14)	1.4			SS	−19 44 31	(0.12)	0.7	12.4		SS	−18 21 15	0.6	0.8	12.8
	260	17 5 10.1	0.7	2.9	0.2		287	17 39 33.4	0.3	9.8	0.1		314	18 8 35.8	0.4	11.3	0.1
	SS	−22 12 56	0.3	0.5	12.8		SS	−19 36 36	0.2	0.6	12.4		SS	−1 50 1	(0.14)	0.6	12.5
	261	17 6 39.2	(0.10)				288	17 40 44.4	0.5	10.3	0.1		315	18 10 24.7	(0.07)		
	SS	−42 33 23	(0.13)				SS	−19 39 52	(0.12)	0.7	12.6		SS	−22 44 23	(0.08)		
	262	17 6 39.8	(0.09)				289	17 40 49.5	0.1	10.3	0.1		316	18 12 13.6	(0.08)		
	SS	−34 13 52	(0.12)				SS	−19 44 20	(0.11)	0.2	11.7		SS	−22 40 20	(0.09)		
	263	17 8 2.3	(0.09)				290	17 41 22.6	0.1	−4.2	0.0		317	18 11 60.0	(0.11)		
	SS	−32 2 52	(0.12)				SS	−19 47 39	(0.13)	1.2	11.8		SS	−7 54 0	(0.14)		
	264	17 8 21.8	0.3	7.3	0.1		291	17 45 20.9	(0.10)				318	18 12 20.7	(0.10)		
	SS	−36 30 51	(0.12)	0.7	12.4		SS	−20 0 30	(0.12)				SS	−22 45 22	(0.11)		
	265	17 8 30.1	0.4	4.8	0.1		292	17 46 23.1	(0.11)				319	18 12 8.5	0.2	4.3	0.1
	SS	−22 53 50	(0.12)	0.4	12.6		SS	−20 6 2	(0.14)				SS	−7 32 43	(0.13)	0.4	12.2
	266	17 8 47.5	(0.09)				293	17 46 47.3	0.8	10.5	0.1		320	18 12 35.6	0.6	12.8	0.1
	SS	−32 6 54	(0.12)				SS	−20 16 37	(0.13)	1.0			SS	−15 49 11	(0.12)	1.0	12.7
	267	17 10 44.3	0.9	6.1	0.2		294	17 47 0.6	0.4	10.6	0.1		321	18 13 53.0	0.3	5.0	0.1
	SS	−40 31 35	0.7	0.7	12.9		SS	−20 30 29	0.4	0.5			SS	−7 4 36	(0.12)	0.5	12.3
	268	17 11 48.6	0.7	4.1	0.1		295	17 47 3.3	(0.10)				322	18 14 5.1	0.4	4.6	0.1
	SS	−22 28 36	(0.13)	1.0	12.7		SS	−20 17 43	(0.12)				SS	−7 8 30	(0.13)	0.6	
	269	17 13 3.7	(0.09)				296	17 51 45.2	0.1	4.2			323	18 14 9.9	0.0	5.0	0.1
	SS	−30 15 43	(0.12)				SS	−2 58 49	(0.13)	0.5	12.0		SS	−6 58 26	(0.12)	0.8	
	270	17 13 29.1	0.4	9.4	0.1		297	17 53 16.6	0.4	6.6	0.1		324	18 14 28.0	(0.11)		
	SS	−34 15 23	(0.13)	0.9	12.5		SS	−8 25 1	(0.14)	0.5			SS	−7 7 55	(0.13)		

Table 5. Continued

Nr	α (2000)	2−1	v	τ_{2-1}	Nr	α (2000)	2−1	v	τ_{2-1}	Nr	α (2000)	2−1	v	τ_{2-1}
Obs	δ	3−2	Δv	log N	Obs	δ	3−2	Δv	log N	Obs	δ	3−2	Δv	log N
325	18 14 37.3	0.9	4.9	0.1	352	18 38 8.8	0.4	2.5	0.1	379	19 2 13.7	0.2	16.5	0.1
SS	−7 23 2	(0.13)	0.8	12.9	SS	−13 43 58	(0.11)	0.9	12.5	SS	−4 22 45	(0.12)	0.5	12.3
326	18 14 43.4	(0.11)			353	18 38 55.0	(0.11)			380	19 4 36.7	(0.10)		
SS	7 4 38	(0.14)			SS	13 23 24	(0.16)			SS	−5 21 2	(0.11)		
327	18 15 34.6	1.1	6.5	0.1	354	18 39 20.3	(0.11)			381	19 10 8.4	(0.10)		
SS	−18 11 12	0.4	1.1		SS	13 8 53	(0.15)			SS	−78 36 3	(0.13)		
328	18 15 17.1	0.5	8.1	0.1	355	18 41 36.2	(0.09)			382	19 10 57.1	0.2	19.3	0.1
SS	−3 45 37	0.4	0.6	12.6	SS	−2 9 17	(0.11)			SS	−78 36 5	(0.12)	0.8	12.1
329	18 15 33.4	0.1	−30.7	0.1	356	18 42 28.6	(0.09)			383	19 6 12.5	0.9	12.3	0.1
SS	−16 26 10	(0.12)	0.7		SS	−19 59 14	(0.11)			SS	−6 53 27	0.7	1.1	12.9
330	18 15 49.2	0.3	8.1	0.1	357	18 47 18.9	0.4	10.5	0.1	384	19 12 13.1	(0.13)		
SS	−3 51 11	(0.11)	1.1		SS	−4 33 6	0.2	0.4	12.5	SS	17 57 51	(0.14)		
331	18 15 49.1	1.0	7.6	0.2	358	18 48 56.5	0.1	3.6	0.0	385	19 13 20.8	(0.12)		
SS	−3 44 28	0.9	0.7		SS	−5 4 52	(0.11)	0.8		SS	16 34 39	(0.14)		
332	18 16 14.7	0.7	7.6	0.1	359	18 53 2.7	(0.10)			386	19 13 53.0	0.2	6.1	0.2
SS	−2 32 47	0.5	0.9		SS	−6 59 1	(0.12)			OK	16 27 25	0.2	0.3	12.2
333	18 16 59.4	0.9	6.6	0.2	360	18 53 20.3	0.2	−11.0	0.1	387	19 15 56.2	(0.10)		
SS	−18 2 44	0.5	1.0		SS	−6 39 32	(0.11)	0.7	12.3	SS	−1 19 7	(0.11)		
334	18 19 46.8	0.2	6.8	0.0	361	18 53 22.5	(0.10)			388	19 16 7.1	(0.10)		
SS	−6 5 51	(0.12)	1.3		SS	−6 46 14	(0.12)			SS	−1 16 19	(0.13)		
335	18 22 29.4	(0.10)			362	18 53 40.2	0.0	−11.3	0.0	389	19 20 16.8	0.8	6.6	0.1
SS	−1 27 32	(0.12)			SS	−7 25 30	(0.12)	0.6		OK	11 36 12	0.9	1.1	12.9
336	18 22 44.7	0.2	8.6	0.1	363	18 53 56.2	0.2	12.5	0.1	390	19 20 30.9	1.6	7.2	0.3
SS	−1 42 40	(0.13)	0.4		SS	−7 26 29	(0.12)	0.5	12.2	SS	11 30 37	0.9	0.8	13.2
337	18 23 31.9	(0.10)			364	18 54 24.0	(0.10)			391	19 20 47.5	0.1	10.8	0.1
SS	−20 45 38	(0.11)			SS	−7 13 51	(0.13)			OK	23 29 34	(0.14)	0.4	11.7
338	18 23 46.2	(0.11)			365	18 54 34.9	(0.10)			392	19 23 20.0	0.2	6.5	0.1
SS	−1 17 31	(0.14)			SS	−4 33 17	(0.14)			SS	12 25 52	0.3	0.5	12.2
339	18 24 18.8	0.4	8.7	0.1	366	18 54 51.0	(0.10)			393	19 23 51.5	(0.11)		
SS	0 58 53	(0.13)	0.9		SS	−4 36 3	(0.13)			SS	11 7 1	(0.15)		
340	18 24 57.5	(0.10)			367	18 55 44.8	(0.10)			394	19 26 32.5	1.7	10.2	0.3
SS	−10 53 0	(0.11)			SS	−4 26 29	(0.12)			OK	23 58 42	0.8	0.8	13.2
341	18 25 30.2	0.4	5.6	0.1	368	18 56 47.1	(0.10)			395	19 29 55.7	(0.11)		
SS	−10 39 55	(0.11)	0.5		SS	−4 45 26	(0.12)			SS	14 34 40	(0.15)		
342	18 26 14.8	0.3	5.7	0.1	369	18 57 32.1	(0.10)			396	19 34 47.4	0.4	9.9	0.1
SS	−10 18 12	(0.11)	0.5		SS	−4 44 16	(0.11)			SS	12 14 30	(0.15)	0.7	12.5
343	18 27 51.2	(0.09)			370	18 58 59.9	(0.10)			397	19 35 15.4	(0.12)		
SS	−11 27 31	(0.11)			SS	−4 32 30	(0.12)			SS	12 19 47	(0.18)		
344	18 29 53.9	(0.09)			371	18 59 24.8	(0.10)			398	19 36 6.4	(0.09)		
SS	−13 41 15	(0.11)			SS	−4 30 49	(0.11)			SS	18 23 36	(0.12)		
345	18 29 57.0	21.0	7.6	1.7	372	19 1 51.3	10.8	5.6	2.5	399	19 36 35.4	(0.11)		
OK	1 13 15	15.0	3.3	14.5	SS	−36 58 52	9.0	1.5		S	12 19 39			
346	18 30 28.9	(0.10)			373	19 1 31.9	0.5	10.3	0.1	400	19 37 1.0	1.7	8.3	0.3
SS	−17 42 53	(0.11)			SS	−5 27 20	(0.11)	1.1		OK	7 34 11	1.4	0.9	13.2
347	18 30 40.8	(0.09)			374	19 1 40.9	(0.10)			401	19 41 30.7	(0.12)		
SS	−16 5 21	(0.11)			SS	−4 33 58	(0.12)			SS	11 13 60	(0.14)		
348	18 32 24.4	(0.04)			375	19 1 44.8	(0.10)			402	19 42 10.6	(0.12)		
SS	−9 10 30	(0.11)			SS	−5 21 44	(0.12)			SS	11 22 4	(0.14)		
349	18 32 32.1	0.3	4.5	0.0	376	19 1 46.0	0.4	−0.0	0.1	403	19 42 31.1	(0.19)		
SS	−8 57 44	(0.11)	1.2	12.3	SS	−5 32 51	(0.12)	0.6		OK	18 52 9	(0.13)		
350	18 32 52.5	0.2	4.9	0.1	377	19 1 58.0	(0.10)			404	19 43 55.9	(0.13)		
SS	−9 13 50	(0.11)	0.4	12.1	SS	−5 33 57	(0.12)			SS	19 4 60	(0.14)		
351	18 33 18.0	0.5	6.4	0.1	378	19 2 5.7	0.3	10.0	0.1	405	19 44 40.6	(0.11)		
SS	−26 1 34	(0.12)	0.5	12.6	SS	−5 17 51	(0.12)	0.6	12.4	S	8 37 48			

Table 5. Continued

Nr Obs	α (2000) δ	2−1 3−2	v Δv	τ_{2-1} log N
406	19 45 27.0	1.9	15.8	0.2
OK	27 52 21	0.7	1.6	13.2
407	19 46 30.5	(0.21)		
OK	21 13 32	(0.13)		
408	19 54 40.5	(0.14)		
O	33 47 23			
409	19 59 46.8	0.9	24.3	0.2
OK	24 55 29	0.7	0.9	12.9
410	20 1 31.2	(0.18)		
OK	24 42 47	(0.14)		
411	20 3 60.0	0.5	8.9	0.2
OK	26 39 17	0.2	0.4	12.7
412	20 4 14.8	(0.21)		
OK	26 46 1	(0.14)		
413	20 7 6.7	10.5	6.0	0.5
OK	27 28 53	8.3	3.8	14.0
414	20 7 44.8	(0.17)		
O	37 5 54			
415	20 18 18.8	(0.12)		
O	63 52 39			
416	20 23 19.9	1.0	3.2	0.3
OK	68 1 55	0.4	0.4	13.0
417	20 31 42.0	(0.12)		
O	25 59 51			
418	20 33 30.5	0.3	−2.8	0.2
OK	64 1 28	(0.14)	0.4	12.4
419	20 34 46.2	(0.12)		
OK	64 10 45	(0.16)		
420	20 35 50.2	1.3	2.6	0.3
OK	67 54 22	0.6	0.8	13.1
421	20 36 17.1	1.4	−2.8	0.2
OK	63 53 15	0.8	1.1	13.1
422	20 37 51.4	(0.11)		
OK	56 18 20	(0.11)		
423	20 43 29.9	1.7	2.6	0.3
O	67 52 42		0.9	13.2
424	20 48 18.2	0.4	−2.0	0.1
OK	59 38 22	(0.13)	0.4	
425	20 49 18.9	(0.11)		
O	59 31 13			
426	20 50 43.1	4.5	−2.3	0.5
OK	44 21 59	3.2	1.8	13.6
427	20 51 20.4	0.4	−1.6	0.1
OK	56 15 45	(0.12)	0.5	12.5
428	20 51 27.4	0.8	−2.8	0.2
OK	60 18 60	0.2	0.7	12.8
429	20 53 29.6	1.4	−2.3	0.3
OK	60 14 40	0.6	0.8	13.1
430	20 53 50.3	1.3	−2.5	0.3
OK	60 9 46	0.9	0.7	13.1
431	20 53 32.1	0.5	3.5	0.2
OK	68 18 27	0.1	0.5	
432	21 0 22.4	2.0	2.9	0.3
OK	68 12 53	1.1	1.1	13.3
433	21 2 24.0	1.3	2.7	0.2
OK	67 54 8	0.5	1.0	13.0
434	21 12 20.1	0.7	2.9	0.1
OK	47 24 24	(0.13)	0.7	12.8
435	21 17 40.8	1.0	2.6	0.4
OK	68 18 23	0.8	0.4	13.0
436	21 32 23.7	0.2	2.4	0.1
OK	57 24 8	(0.12)	0.2	
437	21 33 12.1	1.1	−5.7	0.2
OK	57 29 34	0.8	1.0	13.0
438	21 33 32.3	1.5	−5.3	0.3
OK	58 3 28	0.5	0.8	13.1
439	21 33 55.5	(0.25)		
O	54 41 29			
440	21 36 5.4	0.6	−4.1	0.1
OK	58 31 39	(0.12)	0.9	12.7
441	21 36 12.3	4.4	−8.1	0.5
OK	57 27 34	3.1	1.4	13.7
442	21 37 13.8	1.1	12.6	0.2
OK	43 21 34	0.4	0.9	13.0
443	21 40 28.9	1.6	0.9	0.2
OK	56 35 58	0.8	1.1	13.1
444	21 40 33.0	0.5	−0.9	0.1
OK	57 48 6	(0.11)	0.7	12.6
445	21 40 42.3	17.4	0.6	1.5
OK	58 16 10	17.1	2.9	14.4
446	21 40 33.4	(0.14)		
OK	70 18 33	(0.13)		
447	21 46 6.7	4.1	−1.7	0.6
OK	57 26 23	1.6	1.2	13.6
448	21 46 14.6	0.8	−2.5	0.2
OK	57 8 59	0.3	0.7	12.9
449	21 46 29.2	1.7	−3.1	0.2
OK	57 18 41	0.9	1.2	13.2
450	21 46 36.7	(0.30)		
OK	57 12 25	(0.12)		
451	21 47 25.7	2.5	4.2	0.3
OK	47 32 10	2.3	1.4	13.4
452	21 56 18.4	(0.16)		
OK	59 1 10	(0.12)		
453	22 5 25.1	(0.13)		
OK	59 33 33	(0.12)		
454	22 7 21.7	(0.19)		
OK	59 40 15	(0.12)		
455	22 13 22.5	1.1	0.2	0.3
OK	41 1 31	0.4	0.5	13.0
456	22 9 56.6	(0.15)		
O	86 44 3			
457	22 28 52.2	7.9	−10.1	0.8
OK	64 13 43	4.8	2.0	14.0
458	22 30 31.7	1.1	−4.1	0.2
OK	75 14 17	0.9	0.6	13.0
459	22 31 18.8	1.0	−4.4	0.3
OK	75 13 18	0.7	0.6	13.0
460	22 33 48.3	0.4	−3.7	0.1
OK	58 33 30	(0.13)	0.5	
461	22 47 48.7	2.2	−41.8	0.2
O	58 2 50		1.4	13.3
462	23 11 41.8	0.8	−7.9	0.2
OK	66 3 7	0.1	0.5	12.8
463	23 11 57.5	0.2	−11.2	0.1
OK	61 39 4	(0.11)	0.5	
464	23 25 12.8	1.3	−11.0	0.3
OK	63 36 30	0.6	0.7	13.1
465	23 25 29.6	1.7	4.0	0.5
OK	74 18 15	0.8	0.6	13.2
466	23 25 48.7	1.9	4.2	0.4
OK	74 17 37	1.0	0.7	13.3
467	23 55 21.9	(0.15)		
O	58 51 22			
468	23 56 43.5	1.0	−0.7	0.3
OK	58 34 29	0.6	0.5	13.0
469	23 57 25.3	(0.12)		
O	64 49 27			
470	23 59 25.7	3.1	−13.1	0.3
OK	67 23 39	2.1	1.5	13.5
471	0 1 49.9	0.2	−9.4	
OK	48 6 8	0.0	0.5	12.1

Description of the table:
Column 1: A small 9 point, 1′ spacings, map per core, where large filled dots refer to the position of maximum CS (2-1) emission, small filled dots to emission above the 50% level of the maximum. Small open symbols denote positions with emission above the 3σ level. Blanks are non-detections.
Column 2: In the upper row a running number is given, and in the lower the observatories are identified: O = OSO, K = Kitt Peak, S = SEST.
Columns 3 − 5: Right Ascension and Declination of epoch J2000 are given in the upper and lower row, respectively.
Column 6: The integrated line intensity $\int T_{\rm mb} dv$ in K km s^{-1} is given for CS (2-1) in the upper row, and for CS (3-2) in the lower. For non-detections, the $T_{\rm mb}$-rms value (in K) is given in parentheses.
Column 7: The LSR-velocity (upper) and line width (lower) in km s^{-1} of the CS (2-1) line.
Column 8: The optical depth (upper) in the CS (2-1) line and the total CS column density in cm^{-2} (lower).

Table 6. Core IDs, Coordinates, References and Observatories

Nr	RA (J2000) h m s	Dec (J2000) ° ′ ″	Name	Cat	Observatory CS (2-1)	Observatory CS (3-2)
1	0 3 58.66	68 34 40.9	Sug2 HII(NGC7822)	S91	OSO 97	KITT 97
2	0 5 24.43	67 17 38.9	Sug3 HII(NGC7822)	S91	OSO 97	KITT 97
3	0 14 41.67	64 9 40.3	CB1 KHAV3	Cle	OSO 97	no
4	0 19 4.16	63 55 31.0	CB2 L1281	Cle	OSO 97	KITT 97
5	0 28 45.75	56 42 7.9	CB3 LBN594	Cle	OSO 97	no
6	0 39 3.04	52 51 28.5	CB4 DC	Cle	OSO 98	KITT 97
7	0 44 6.28	62 30 1.7	CB5 L1301	Cle	OSO 98	KITT 97
8	0 49 28.62	50 44 41.1	CB6 LBN613	Cle	OSO 98	KITT 97
9	0 59 4.03	60 53 31.6	Sug4 HII(S185)	S91	OSO 97	no
10	1 12 15.79	64 25 54.8	CB7	Cle	OSO 97	KITT 97
11	1 23 56.58	74 22 30.6	CB8	Cle	OSO 97	KITT 97
12	1 29 51.81	63 5 28.8	CB9 L1325	Cle	OSO 97	no
13	1 30 50.09	67 23 46.3	CB10	Cle	OSO 97	KITT 97
14	1 37 2.33	65 2 42.7	CB11	Cle	OSO 97	KITT 97
15	1 38 37.33	65 5 13.9	CB12	Cle	OSO 98	KITT 97
16	1 56 54.64	62 41 18.3	CB13 L1345	Cle	OSO 97	KITT 97
17	1 57 35.90	62 39 36.8	CB14 L1346	Cle	OSO 97	KITT 97
18	2 29 1.70	61 33 32.5	Sug5 HII(S190)	S91	OSO 97	no
19	2 34 44.99	60 47 48.3	Sug6 HII(S190)	S91	OSO 97	no
20	2 34 52.08	61 46 47.0	Sug7 HII(S190)	S91	OSO 97	no
21	2 35 37.37	61 19 36.0	Sug8 HII(S190)	S91	OSO 97	no
22	2 36 27.12	61 23 36.7	Sug9 HII(S190)	S91	OSO 97	no
23	2 48 15.33	60 24 35.5	Sug10 HII(S199)	S91	OSO 97	no
24	2 51 28.93	60 3 14.1	Sug11 HII(S199)	S91	OSO 97	no
25	2 55 2.90	60 35 44.6	Sug12 HII(S199)	S91	OSO 97	no
26	3 1 0.67	60 40 20.5	Sug13 HII(S199)	S91	OSO 97	no
27	3 1 32.24	60 29 11.9	Sug14 HII(S199)	S91	OSO 97	no
28	3 56 36.47	56 8 2.2	CB15 B6,L1387	Cle	OSO 97	KITT 97
29	4 3 18.27	56 50 8.1	CB16 L1388	Cle	OSO 97	KITT 97
30	4 4 37.90	56 56 11.1	CB17 L1389	Cle	OSO 97	KITT 97
31	4 5 0.55	60 32 19.1	CB18	Cle	OSO 97	KITT 97
32	4 4 47.46	26 19 41.6	L1489	BM	OSO 97	no
33	4 25 10.46	54 19 10.8	L14G	BM	OSO 97	KITT 97
34	4 30 52.03	54 51 55.1	L14K	BM	OSO 97	KITT 97
35	4 58 29.59	52 15 41.0	CB24	Cle	OSO 97	KITT 97
36	4 59 4.05	52 3 23.6	CB25 L1437	Cle	OSO 97	KITT 97
37	5 0 9.24	52 4 60.0	CB26 L1439	Cle	OSO 97	KITT 97
38	5 4 9.71	32 43 8.6	L1512	BM	OSO 97	no
39	5 4 15.33	32 47 29.2	CB27 SCHO93	Cle	OSO 97	no
40	5 6 20.19	-3 56 2.2	CB28 LBN923	Cle	SEST 96	SEST 96
41	5 22 11.41	-3 41 34.1	CB29	Cle	SEST 96	SEST 96
42	5 23 30.06	33 11 54.0	Sug15 HII(S236)	S91	OSO 97	no
43	5 29 44.33	5 45 2.7	CB30	Cle	OSO 98	KITT 97
44	5 44 29.70	9 8 53.7	B35A,Sug18	BM	OSO 98	KITT 97
45	5 46 36.94	20 45 31.0	CB33	Cle	OSO 98	KITT 97
46	6 0 38.88	31 39 30.3	CB37 L1555	Cle	OSO 97	KITT 97
47	6 0 56.04	16 56 50.3	CB38	Cle	OSO 98	KITT 97
48	6 3 11.63	16 37 6.4	CB43	Cle	OSO 98	KITT 97
49	6 8 55.18	17 50 19.4	CB45 L1578(?)	Cle	OSO 98	KITT 97
50	6 22 58.66	23 9 58.3	Sug23 HII(S249)	S91	OSO 97	KITT 97
51	6 48 42.87	-16 53 26.6	CB52	Cle	SEST 96	SEST 96
52	7 4 16.80	-16 24 32.6	CB54 LBN1042	Cle	SEST 96	SEST 96
53	7 4 44.59	-16 35 41.6	CB55	Cle	SEST 96	SEST 96
54	7 14 35.99	-25 8 54.1	CB56	Cle	SEST 96	SEST 96
55	7 17 33.92	-23 1 35.3	CB57	Cle	SEST 96	SEST 96
56	7 18 2.21	-23 35 6.3	CB58-1	Cle	SEST 96	SEST 96
57	7 18 13.14	-23 38 52.0	CB58	Cle	SEST 96	SEST 96
58	7 18 15.08	-23 41 42.2	CB58-2	Cle	SEST 96	SEST 96

Nr	RA (J2000) h m s	Dec (J2000) ° ′ ″	Name	Cat	Observatory CS (2-1)	Observatory CS (3-2)
59	7 19 31.08	3 56 50.7	CB59	Cle	OSO 97	no
60	7 29 32.68	-41 10 30.3	DC 253.8-10.9	Har	SEST 96	SEST 96
61	7 40 47.32	-41 26 57.3	DC 255.1-9.2	Har	SEST 96	SEST 96
62	7 40 51.72	-43 49 9.7	DC 257.2-10.3	Har	SEST 96	SEST 96
63	7 42 30.31	-42 5 10.1	DC 255.8-9.2	Har	SEST 96	SEST 96
64	7 42 48.69	-42 25 47.3	DC 256.1-9.3	Har	SEST 96	SEST 96
65	7 43 5.30	-42 7 30.4	DC 255.9-9.1	Har	SEST 96	SEST 96
66	7 43 34.90	-42 22 2.4	DC 256.1-9.1	Har	SEST 96	SEST 96
67	7 45 10.38	-34 36 14.2	DC 249.4-5.1	Har	SEST 96	SEST 96
68	8 4 35.64	-31 30 46.6	CB60 L1670	Cle	SEST 96	SEST 96
69	8 5 26.26	-39 8 56.1	DC 255.4-3.9	Har	SEST 96	SEST 96
70	8 9 31.58	-36 4 47.2	DC 253.3-1.6	Har	SEST 96	SEST 96
71	8 10 9.54	-38 43 25.6	DC 255.6-2.9	Har	SEST 96	SEST 96
72	8 12 21.03	-33 56 15.5	DC 251.8+0.0	Har	SEST 96	SEST 96
73	8 12 22.92	-34 1 3.6	DC 251.9+0.0	Har	SEST 96	SEST 96
74	8 12 25.29	-33 45 39.7	DC 251.7+0.2	Har	SEST 96	SEST 96
75	8 12 22.64	-38 50 3.8	DC 255.9-2.6	Har	SEST 96	SEST 96
76	8 14 21.42	-34 30 52.8	DC 252.5+0.1	Har	SEST 96	SEST 96
77	8 14 35.47	-42 5 12.1	DC 258.9-4.1	Har	SEST 96	SEST 96
78	8 14 34.81	-44 5 54.1	DC 260.5-5.2	Har	SEST 96	SEST 96
79	8 15 7.23	-38 41 1.8	DC 256.1-2.1	Har	SEST 96	SEST 96
80	8 15 28.17	-34 4 44.9	DC 252.3+0.5	Har	SEST 96	SEST 96
81	8 15 59.55	-33 50 46.8	DC 252.2+0.7	Har	SEST 96	SEST 96
82	8 16 37.69	-42 7 55.5	DC 259.1-3.8	Har	SEST 96	SEST 96
83	8 16 35.63	-52 54 32.0	DC 268.2-9.7	Har	SEST 96	SEST 96
84	8 17 10.58	-39 52 57.3	DC 257.3-2.5	Har	SEST 96	SEST 96
85	8 17 12.25	-52 43 22.2	DC 268.1-9.5	Har	SEST 96	SEST 96
86	8 18 39.87	-49 43 51.3	DC 265.7-7.7	Har	SEST 96	SEST 96
87	8 19 15.71	-42 54 47.0	DC 260.0-3.8	Har	SEST 96	SEST 96
88	8 20 33.41	-50 5 34.1	DC 266.1-7.7	Har	SEST 96	SEST 96
89	8 21 20.88	-52 26 25.1	DC 268.2-8.9	Har	SEST 96	SEST 96
90	8 25 44.28	-51 2 4.5	DC 267.4-7.5	Har	SEST 96	SEST 96
91	8 26 11.89	-51 39 18.2	DC 267.9-7.8	Har	SEST 96	SEST 96
92	8 26 34.32	-50 39 55.4	DC 267.2-7.2	Har	SEST 96	SEST 96
93	8 26 39.49	-51 1 37.8	DC 267.5-7.4	Har	SEST 96	SEST 96
94	8 32 0.75	-50 32 50.4	DC 267.6-6.4	Har	SEST 96	SEST 96
95	8 32 42.52	-39 25 4.2	DC 258.6+0.3	Har	SEST 96	SEST 96
96	8 36 54.11	-48 3 30.9	DC 266.0-4.3	Har	SEST 96	SEST 96
97	8 37 18.25	-36 37 55.8	DC 256.9+2.6	Har	SEST 96	SEST 96
98	8 44 13.92	-59 54 2.3	DC 276.2-10.6	Har	SEST 96	SEST 96
99	8 52 38.23	-50 40 4.9	DC 269.7-3.9	Har	SEST 96	SEST 96
100	8 52 35.63	-51 51 52.8	DC 270.6-4.7	Har	SEST 96	SEST 96
101	8 53 15.10	-41 52 24.4	DC 263.0+1.8	Har	SEST 96	SEST 96
102	8 53 25.00	-41 57 19.0	DC 263.1+1.8	Har	SEST 96	SEST 96
103	8 53 42.50	-44 48 2.0	DC 265.3-0.0	Har	SEST 96	SEST 96
104	8 56 37.53	-46 51 35.3	DC 267.2-0.0	Har	SEST 96	SEST 96
105	8 57 27.51	-46 58 20.0	DC 267.4-0.9	Har	SEST 96	SEST 96
106	8 57 34.06	-46 40 44.3	DC 267.1-0.7	Har	SEST 96	SEST 96
107	9 13 24.75	-40 29 32.0	DC 264.5+5.6	Har	SEST 96	SEST 96
108	9 13 50.00	-40 21 39.2	DC 264.4+5.7	Har	SEST 96	SEST 96
109	9 15 32.15	-41 13 32.1	DC 265.3+5.3	Har	SEST 96	SEST 96
110	9 16 9.15	-41 18 57.9	DC 265.4+5.4	Har	SEST 96	SEST 96
111	9 18 47.45	-44 19 11.5	DC 267.9+3.6	Har	SEST 96	SEST 96
112	9 25 44.75	-48 23 37.1	DC 271.6+1.6	Har	SEST 96	SEST 96
113	9 26 7.08	-48 15 2.1	DC 271.6+1.7	Har	SEST 96	SEST 96
114	9 27 14.31	-48 16 47.1	DC 271.7+1.8	Har	SEST 96	SEST 96
115	9 27 33.96	-48 32 54.0	DC 272.0+1.7	Har	SEST 96	SEST 96
116	9 28 21.15	-48 33 14.1	DC 272.1+1.8	Har	SEST 96	SEST 96

Nr	RA (J2000) h m s	Dec (J2000) ° ′ ″	Name	Cat	Observatory CS (2-1)	Observatory CS (3-2)
117	9 28 46.96	-51 36 39.4	DC 274.2-0.4	Har	SEST 96	SEST 96
118	9 29 7.37	-48 32 34.2	DC 272.2+1.9	Har	SEST 96	SEST 96
119	9 31 2.71	-48 38 21.3	DC 272.5+2.0	Har	SEST 96	SEST 96
120	9 36 43.86	-48 51 54.2	DC 273.3+2.5	Har	SEST 96	SEST 96
121	9 38 53.16	-51 28 41.8	DC 275.3+0.8	Har	SEST 96	SEST 96
122	9 45 1.13	-48 51 20.9	DC 274.3+3.4	Har	SEST 96	SEST 96
123	9 45 26.48	-50 38 34.0	DC 275.5+2.1	Har	SEST 96	SEST 96
124	9 45 52.18	-48 18 11.0	DC 274.1+3.9	Har	SEST 96	SEST 96
125	10 25 27.19	-59 25 10.4	DC 285.3-1.6	Har	SEST 96	SEST 96
126	10 36 0.06	-61 7 34.0	DC 287.3-2.4	Har	SEST 96	SEST 96
127	10 38 12.72	-60 11 43.4	DC 287.1-1.5	Har	SEST 96	SEST 96
128	10 43 22.07	-60 15 3.1	DC 287.7-1.2	Har	SEST 96	SEST 96
129	10 48 59.47	-62 23 5.0	DC 289.3-2.8	Har	SEST 96	SEST 96
130	11 4 43.62	-58 10 59.9	DC 289.2+1.8	Har	SEST 96	SEST 96
131	11 14 28.60	-60 53 3.4	DC 291.4-0.2	Har	SEST 96	SEST 96
132	11 27 51.49	-62 9 55.5	DC 293.3-0.9	Har	SEST 96	SEST 96
133	11 29 33.42	-60 42 26.5	DC 293.1+0.6	Har	SEST 96	SEST 96
134	11 29 56.44	-60 58 14.7	DC 293.2+0.4	Har	SEST 96	SEST 96
135	11 30 10.39	-61 13 20.9	DC 293.3+0.1	Har	SEST 96	SEST 96
136	11 32 2.15	-64 23 16.0	DC 294.5-2.8	Har	SEST 96	SEST 96
137	11 33 51.92	79 30 39.3	CB61	Cle	OSO 97	no
138	11 34 44.63	-64 34 41.4	DC 294.8-2.9	Har	SEST 96	SEST 96
139	11 37 32.97	-61 44 36.7	DC 294.3-0.1	Har	SEST 96	SEST 96
140	11 42 50.80	-61 44 20.8	DC 294.9+0.1	Har	SEST 96	SEST 96
141	11 43 31.14	-59 2 33.0	DC 294.3+2.7	Har	SEST 96	SEST 96
142	11 48 0.66	-61 26 4.4	DC 295.4+0.5	Har	SEST 96	SEST 96
143	11 48 9.72	-61 30 34.4	DC 295.5+0.4	Har	SEST 96	SEST 96
144	11 51 28.58	-61 2 53.1	DC 295.7+0.0	Har	SEST 96	SEST 96
145	12 3 57.02	-60 1 54.0	DC 297.0+2.3	Har	SEST 96	SEST 96
146	12 6 16.20	-60 9 11.8	DC 297.3+2.2	Har	SEST 96	SEST 96
147	12 7 8.36	-65 18 41.7	DC 298.3-2.8	Har	SEST 96	SEST 96
148	12 22 8.45	-66 27 7.9	DC 300.0-3.7	Har	SEST 96	SEST 96
149	12 32 27.26	-70 45 14.9	DC 301.4-7.9	Har	SEST 96	SEST 96
150	12 34 21.40	-70 28 49.7	DC 301.5-7.7	Har	SEST 96	SEST 96
151	12 36 18.61	-63 12 36.4	DC 301.2-0.4	Har	SEST 96	SEST 96
152	12 37 8.90	-69 59 53.9	DC 301.7-7.2	Har	SEST 96	SEST 96
153	12 39 39.77	-65 26 28.2	DC 301.7-2.6	Har	SEST 96	SEST 96
154	12 41 1.45	-80 19 45.4	DC 302.5-17.5	Har	SEST 96	SEST 96
155	12 40 54.61	-69 52 15.3	DC 302.0-7.0	Har	SEST 96	SEST 96
156	12 47 50.79	-69 14 51.7	DC 302.6-6.4	Har	SEST 96	SEST 96
157	12 48 46.03	-79 39 21.1	DC 302.8-16.8	Har	SEST 96	SEST 96
158	12 50 24.39	-79 38 13.7	DC 302.9-16.8	Har	SEST 96	SEST 96
159	12 58 54.80	-61 20 16.8	DC 303.8+1.5	Har	SEST 96	SEST 96
160	13 3 14.73	-77 23 0.4	DC 303.6-14.5	Har	SEST 96	SEST 96
161	13 5 24.34	-77 40 45.9	DC 303.7-14.8	Har	SEST 96	SEST 96
162	13 5 53.33	-77 52 45.3	DC 303.7-15.0	Har	SEST 96	SEST 96
163	13 6 30.27	-78 2 20.6	DC 303.7-15.2	Har	SEST 96	SEST 96
164	13 19 31.33	-62 33 26.7	DC 306.2+0.1	Har	SEST 96	SEST 96
165	13 24 32.33	-57 17 1.1	DC 307.4+5.3	Har	SEST 97	SEST 97
166	13 25 48.55	-59 42 53.2	DC 307.3+2.9	Har	SEST 98	SEST 98
167	13 28 51.99	-62 27 30.4	DC 307.2+0.1	Har	SEST 96	SEST 96
168	13 30 2.82	79 22 34.1	CB62	Cle	OSO 97	no
169	14 13 18.65	-57 37 43.4	DC 313.7+3.5	Har	SEST 97	SEST 97
170	14 26 57.91	-55 27 33.5	DC 316.3+4.9	Har	SEST 97	SEST 97
171	14 53 21.35	-61 36 2.7	DC 316.9-2.1	Har	SEST 96	SEST 96
172	14 56 35.12	-56 29 46.7	DC 319.6+2.3	Har	SEST 97	SEST 97
173	15 0 19.63	-56 59 35.3	DC 319.8+1.6	Har	SEST 97	SEST 97
174	15 2 56.24	-63 42 33.9	DC 316.9-4.5	Har	SEST 96	SEST 96

Nr	RA (J2000) h m s	Dec (J2000) ° ′ ″	Name	Cat	Observatory CS (2-1)	Observatory CS (3-2)
175	15 3 37.07	-64 31 49.9	DC 316.6-5.2	Har	SEST 96	SEST 96
176	15 5 11.99	-64 7 56.9	DC 316.9-4.9	Har	SEST 96	SEST 96
177	15 11 13.39	-53 18 24.9	DC 323.0+4.0	Har	SEST 97	SEST 97
178	15 15 13.55	-60 13 36.5	DC 319.9-2.2	Har	SEST 96	SEST 96
179	15 17 31.60	-62 39 29.2	DC 318.8-4.4	Har	SEST 96	SEST 96
180	15 17 12.76	-50 36 41.3	DC 325.2+5.8	Har	SEST 97	SEST 97
181	15 21 1.75	-50 12 16.6	DC 325.9+5.9	Har	SEST 97	SEST 97
182	15 21 35.46	-59 35 51.5	DC 320.9-2.1	Har	SEST 96	SEST 96
183	15 24 30.85	-63 3 24.0	DC 319.3-5.2	Har	SEST 96	SEST 96
184	15 25 2.78	-61 1 40.0	DC 320.5-3.5	Har	SEST 96	SEST 96
185	15 25 45.36	-61 7 7.6	DC 320.5-3.6	Har	SEST 96	SEST 96
186	15 26 26.81	-61 55 59.4	DC 320.1-4.3	Har	SEST 96	SEST 96
187	15 26 17.45	-49 59 28.9	DC 326.8+5.6	Har	SEST 98	SEST 98
188	15 27 11.95	-62 23 14.9	DC 319.9-4.8	Har	SEST 96	SEST 96
189	15 27 2.66	-50 0 38.3	DC 326.9+5.5	Har	SEST 97	SEST 97
190	15 45 35.85	-34 38 56.3	DC 339.0+15.8	Har	SEST 98	SEST 98
191	15 50 16.65	-45 30 27.8	DC 332.7+6.8	Har	SEST 97	SEST 97
192	15 50 48.65	-4 6 14.2	CB63 LBN11	Cle	SEST 97	SEST 97
193	15 53 36.26	-4 35 25.9	L134A	BM	SEST 97	SEST 97
194	15 54 12.12	-2 49 41.7	L183B	BM	SEST 97	SEST 97
195	16 1 8.30	-53 46 30.0	DC 328.7-0.7	Har	SEST 97	SEST 97
196	16 0 10.07	-1 26 44.3	CB64 LBN37	Cle	SEST 97	SEST 97
197	16 2 49.21	-42 13 40.8	DC 336.6+7.8	Har	SEST 97	SEST 97
198	16 3 15.05	-42 6 27.2	DC 336.7+7.8	Har	SEST 97	SEST 97
199	16 4 28.81	-39 37 46.4	DC 338.6+9.5	Har	SEST 97	SEST 97
200	16 9 17.31	-41 49 58.1	DC 337.7+7.3	Har	SEST 97	SEST 97
201	16 10 41.56	-37 52 22.4	DC 340.7+0.0	Har	SEST 97	SEST 97
202	16 12 43.20	-52 15 33.6	DC 331.0-0.7	Har	SEST 97	SEST 97
203	16 18 46.46	-36 42 38.9	DC 342.7+9.7	Har	SEST 97	SEST 97
204	16 20 4.44	-53 18 22.9	DC 331.1-2.3	Har	SEST 97	SEST 97
205	16 19 40.02	-38 11 41.4	DC 341.7+8.5	Har	SEST 97	SEST 97
206	16 22 37.18	-40 23 11.9	DC 340.6+6.6	Har	SEST 97	SEST 97
207	16 23 37.81	-49 32 56.5	DC 334.2+0.0	Har	SEST 97	SEST 97
208	16 26 5.15	-41 15 22.1	DC 340.4+5.5	Har	SEST 98	SEST 98
209	16 26 12.04	-38 25 9.5	DC 342.5+7.4	Har	SEST 97	SEST 97
210	16 26 26.36	-24 24 32.8	L1688A(DCO+ 2-1)	Lor	SEST 97	SEST 97
211	16 26 52.95	-24 32 31.1	L1688C(DCO+ 2-1)	Lor	SEST 97	SEST 97
212	16 27 1.89	-24 38 30.5	L1688E(DCO+ 2-1)	Lor	SEST 97	SEST 97
213	16 27 10.41	-24 29 29.9	L1688B1(DCO+ 2-1)	Lor	SEST 97	SEST 97
214	16 27 19.11	-24 24 29.3	L1688B3(DCO+ 2-1)	Lor	SEST 97	SEST 97
215	16 27 27.96	-24 26 28.7	L1688B2(DCO+ 2-1)	Lor	SEST 98	SEST 98
216	16 27 35.63	-24 43 26.2	L1681B	BM	SEST 97	SEST 97
217	16 27 37.21	-24 42 28.1	L1688F(DCO+ 2-1)	Lor	SEST 98	SEST 98
218	16 28 29.14	-24 18 24.6	L1688D(DCO+ 2-1)	Lor	SEST 97	SEST 97
219	16 28 31.35	-24 19 7.5	L1696A	BM	SEST 98	SEST 98
220	16 30 3.69	-39 9 0.1	DC 342.5+6.4	Har	SEST 98	SEST 98
221	16 31 18.69	-23 41 21.2	CB65 L1704	Cle	SEST 97	SEST 97
222	16 31 35.63	-24 1 27.1	L1709B(DCO+ 2-1)	Lor	SEST 97	SEST 97
223	16 32 2.34	-24 56 11.4	L1689S(DCO+ 2-1)	Lor	SEST 97	SEST 97
224	16 32 22.66	-24 28 33.0	IRAS16293	???	SEST 97	SEST 97
225	16 32 42.03	-23 54 8.6	L1709A(DCO+ 2-1)	Lor	SEST 97	SEST 97
226	16 33 26.60	-36 36 34.3	DC 344.8+7.6	Har	SEST 97	SEST 97
227	16 34 33.17	-15 47 10.8	L43	BM	SEST 97	SEST 97
228	16 34 37.47	-15 47 0.5	L43E	BM	SEST 97	SEST 97
229	16 36 40.07	-46 1 15.8	DC 338.2+0.8	Har	SEST 97	SEST 97
230	16 36 50.22	-35 37 8.4	DC 346.0+7.8	Har	SEST 97	SEST 97
231	16 36 51.75	-35 56 32.3	DC 345.8+7.6	Har	SEST 97	SEST 97
232	16 37 16.11	-35 31 36.7	DC 346.1+7.8	Har	SEST 97	SEST 97

Nr	RA (J2000) h m s	Dec (J2000) ° ′ ″	Name	Cat	Observatory CS (2-1)	Observatory CS (3-2)
233	16 37 27.64	-35 13 53.8	DC 346.4+7.9	Har	SEST 97	SEST 97
234	16 37 46.00	-35 26 22.6	DC 346.3+7.8	Har	SEST 97	SEST 97
235	16 38 52.73	-35 49 48.1	DC 346.1+7.3	Har	SEST 97	SEST 97
236	16 39 30.35	-14 5 50.5	66 L121,MBM142	Cle	SEST 97	SEST 97
237	16 44 18.68	-49 14 38.7	DC 336.7-2.3	Har	SEST 97	SEST 97
238	16 45 1.03	-47 45 11.7	DC 337.9-1.4	Har	SEST 97	SEST 97
239	16 44 50.26	-40 23 5.9	DC 343.4+3.5	Har	SEST 97	SEST 97
240	16 46 45.13	-46 27 22.4	DC 339.1-0.8	Har	SEST 98	SEST 98
241	16 46 44.78	-44 30 46.3	DC 340.5+0.5	Har	SEST 97	SEST 97
242	16 47 6.64	-9 35 21.0	L260	BM	SEST 97	SEST 97
243	16 47 23.12	-13 59 21.1	L158	BM	SEST 97	SEST 97
244	16 48 6.81	-10 51 47.9	L234A	BM	SEST 97	SEST 97
245	16 48 8.50	-10 56 57.8	L234E	BM	SEST 97	SEST 97
246	16 49 9.40	-39 45 6.0	DC 344.5+3.2	Har	SEST 97	SEST 97
247	16 50 15.42	-18 6 6.3	L63	BM	SEST 97	SEST 97
248	16 50 33.70	-19 7 50.1	CB67 L31	Cle	SEST 98	SEST 98
249	16 54 32.26	-40 31 7.6	DC 344.5+2.0	Har	SEST 97	SEST 97
250	16 57 16.24	-16 9 21.9	CB68 L146(?)	Cle	SEST 97	SEST 97
251	16 58 41.82	-50 35 45.0	DC 337.1-4.9	Har	SEST 96	SEST 96
252	16 58 25.54	-36 42 15.1	DC 348.0+3.7	Har	SEST 97	SEST 97
253	17 2 20.01	-33 16 34.4	DC 351.2+5.2	Har	SEST 97	SEST 97
254	17 2 42.04	-33 16 59.8	CB69 B49	Cle	SEST 97	SEST 97
255	17 3 0.05	-22 13 39.0	CB70 L4	Cle	SEST 97	SEST 97
256	17 4 26.20	-36 18 49.7	DC 349.0+3.0	Har	SEST 97	SEST 97
257	17 4 26.90	-36 8 25.6	DC 349.2+3.1	Har	SEST 97	SEST 97
258	17 4 45.97	-36 10 18.3	DC 349.2+3.1	Har	SEST 97	SEST 97
259	17 4 48.78	-36 3 36.1	DC 349.3+3.1	Har	SEST 97	SEST 97
260	17 5 10.11	-22 12 55.8	CB71	Cle	SEST 97	SEST 97
261	17 6 39.18	-42 33 22.7	DC 344.3-1.1	Har	SEST 97	SEST 97
262	17 6 39.79	-34 13 52.1	DC 351.0+3.9	Har	SEST 97	SEST 97
263	17 8 2.31	-32 2 52.1	DC 352.9+5.0	Har	SEST 97	SEST 97
264	17 8 21.75	-36 30 51.0	DC 349.3+2.3	Har	SEST 97	SEST 97
265	17 8 30.11	-22 53 49.7	CB72 B57,L11	Cle	SEST 97	SEST 97
266	17 8 47.45	-32 6 53.9	CB73 B56,L1685	Cle	SEST 97	SEST 97
267	17 10 44.33	-40 31 35.2	DC 346.4-0.5	Har	SEST 97	SEST 97
268	17 11 48.64	-22 28 35.6	B74 B60,L38(?)	Cle	SEST 97	SEST 97
269	17 13 3.75	-30 15 42.6	CB75 B247	Cle	SEST 97	SEST 97
270	17 13 29.13	-34 15 23.0	DC 351.8+2.8	Har	SEST 97	SEST 97
271	17 15 2.11	-20 29 59.7	CB76 B61,L111	Cle	SEST 98	SEST 98
272	17 15 30.21	-32 24 56.3	DC 353.5+3.5	Har	SEST 98	SEST 98
273	17 15 14.63	-1 43 20.0	CB77	Cle	SEST 98	SEST 98
274	17 19 35.85	-43 27 3.5	DC 345.0-3.5	Har	SEST 96	SEST 96
275	17 19 43.72	-26 43 1.9	CB79 B65,L1772	Cle	SEST 97	SEST 97
276	17 20 56.20	-33 31 21.0	DC 353.3+1.9	Har	SEST 97	SEST 97
277	17 21 47.49	-44 8 48.1	DC 344.6-4.3	Har	SEST 96	SEST 96
278	17 21 49.98	-21 48 23.6	CB80 L101	Cle	SEST 97	SEST 97
279	17 22 37.33	-27 5 1.4	CB81 L1774	Cle	SEST 97	SEST 97
280	17 22 36.75	-23 50 34.3	CB82 B68,L55	Cle	SEST 97	SEST 97
281	17 25 11.53	-40 16 27.1	DC 348.2-2.6	Har	SEST 96	SEST 96
282	17 30 37.67	-43 8 27.9	DC 346.4-5.0	Har	SEST 96	SEST 96
283	17 32 14.16	-25 25 28.8	CB89 L52	Cle	SEST 96	SEST 96
284	17 35 10.66	-33 32 37.5	DC 354.9-0.6	Har	SEST 96	SEST 96
285	17 35 26.36	-33 21 36.3	DC 355.1-0.5	Har	SEST 96	SEST 96
286	17 38 26.52	-19 44 30.5	CB90 L216(?)	Cle	SEST 96	SEST 96
287	17 39 33.36	-19 36 35.7	CB91 L219	Cle	SEST 96	SEST 96
288	17 40 44.44	-19 39 51.5	CB92 L226	Cle	SEST 96	SEST 96
289	17 40 49.54	-19 44 20.2	CB93 L223	Cle	SEST 96	SEST 96
290	17 41 22.61	-19 47 38.8	CB94 L222	Cle	SEST 96	SEST 96

Nr	RA (J2000) h m s	Dec (J2000) ° ′ ″	Name	Cat	Observatory CS (2-1)	Observatory CS (3-2)
291	17 45 20.94	-20 0 30.5	CB95 B83, L233	Cle	SEST 96	SEST 96
292	17 46 23.07	-20 6 2.0	CB96 L235	Cle	SEST 96	SEST 96
293	17 46 47.31	-20 16 37.2	CB97 B84,L235	Cle	SEST 96	SEST 96
294	17 47 0.62	-20 30 29.3	CB98	Cle	SEST 96	SEST 96
295	17 47 3.34	-20 17 43.1	CB99 L235	Cle	SEST 96	SEST 96
296	17 51 45.16	-2 58 48.8	CB100	Cle	SEST 96	SEST 96
297	17 53 16.56	-8 25 1.4	CB101 L392	Cle	SEST 96	SEST 96
298	17 54 42.93	-27 49 56.0	CB102	Cle	SEST 96	SEST 96
299	17 55 6.42	-32 37 4.6	DC 357.9-3.6	Har	SEST 96	SEST 96
300	17 55 12.17	-34 15 40.2	DC 356.5-4.5	Har	SEST 96	SEST 96
301	17 55 24.96	-2 48 44.8	CB103	Cle	SEST 96	SEST 96
302	17 55 31.38	-8 15 25.5	CB104 L400	Cle	SEST 96	SEST 96
303	17 58 6.09	-3 46 21.1	CB105 L460	Cle	SEST 96	SEST 96
304	18 1 9.78	-32 49 44.1	DC 358.3-4.8	Har	SEST 96	SEST 96
305	18 0 34.79	-3 30 36.2	CB106 L468	Cle	SEST 96	SEST 96
306	18 1 17.02	-32 58 13.6	DC 358.2-4.9	Har	SEST 96	SEST 96
307	18 3 2.48	-46 39 48.9	DC 346.2-11.7	Har	SEST 96	SEST 96
308	18 2 58.01	-27 52 7.9	CB107 B86,L93	Cle	SEST 96	SEST 96
309	18 3 15.10	-33 1 5.0	DC 358.4-5.3	Har	SEST 96	SEST 96
310	18 3 4.13	-20 51 0.1	CB108 L262	Cle	SEST 96	SEST 96
311	18 5 3.85	-28 25 53.8	CB109 SCHO741	Cle	SEST 96	SEST 96
312	18 5 55.94	-18 25 13.5	CB110 L307	Cle	SEST 96	SEST 96
313	18 7 13.85	-18 21 14.8	CB111 L310	Cle	SEST 96	SEST 96
314	18 8 35.83	-1 50 1.1	CB112 L502(?)	Cle	SEST 96	SEST 96
315	18 10 24.67	-22 44 23.1	CB113 L249	Cle	SEST 96	SEST 96
316	18 12 13.57	-22 40 20.2	CB114	Cle	SEST 96	SEST 96
317	18 11 59.95	-7 54 0.5	CB115 L426	Cle	SEST 96	SEST 96
318	18 12 20.68	-22 45 21.7	CB116	Cle	SEST 96	SEST 96
319	18 12 8.53	-7 32 42.9	CB117 L430	Cle	SEST 96	SEST 96
320	18 12 35.61	-15 49 11.2	CB118	Cle	SEST 96	SEST 96
321	18 13 52.98	-7 4 36.2	CB119 L438	Cle	SEST 96	SEST 96
322	18 14 5.05	-7 8 30.4	CB120 L438	Cle	SEST 96	SEST 96
323	18 14 9.85	-6 58 26.0	CB121	Cle	SEST 96	SEST 96
324	18 14 28.04	-7 7 54.7	CB122 L438	Cle	SEST 96	SEST 96
325	18 14 37.34	-7 23 2.0	CB123 L436	Cle	SEST 96	SEST 96
326	18 14 43.42	7 4 38.0	CB124 LBN102	Cle	SEST 97	SEST 97
327	18 15 34.60	-18 11 12.3	CB125 B92,L323	Cle	SEST 96	SEST 96
328	18 15 17.08	-3 45 37.0	CB126 L490(?)	Cle	SEST 96	SEST 96
329	18 15 33.37	-16 26 10.3	CB127	Cle	SEST 96	SEST 96
330	18 15 49.19	-3 51 10.6	CB128 L492	Cle	SEST 96	SEST 96
331	18 15 49.06	-3 44 27.6	CB129 L492	Cle	SEST 96	SEST 96
332	18 16 14.67	-2 32 46.7	CB130 L507(?)	Cle	SEST 96	SEST 96
333	18 16 59.41	-18 2 44.2	CB131 B93,L328	Cle	SEST 96	SEST 96
334	18 19 46.82	-6 5 51.5	CB132 L466	Cle	SEST 96	SEST 96
335	18 22 29.40	-1 27 32.5	CB133	Cle	SEST 96	SEST 96
336	18 22 44.69	-1 42 40.4	CB134	Cle	SEST 96	SEST 96
337	18 23 31.91	-20 45 37.8	CB135 L306	Cle	SEST 96	SEST 96
338	18 23 46.20	-1 17 30.9	CB136 L533	Cle	SEST 96	SEST 96
339	18 24 18.85	0 58 52.5	CB137 L539	Cle	SEST 96	SEST 96
340	18 24 57.48	-10 53 0.1	CB138 L414	Cle	SEST 96	SEST 96
341	18 25 30.21	-10 39 54.7	139 B94,L416,L4	Cle	SEST 96	SEST 96
342	18 26 14.78	-10 18 11.5	140 B96,L420(?)	Cle	SEST 96	SEST 96
343	18 27 51.16	-11 27 30.6	CB141 L411	Cle	SEST 96	SEST 96
344	18 29 53.85	-13 41 14.8	CB142	Cle	SEST 96	SEST 96
345	18 29 57.00	1 13 15.1	Serp SMM4	LLM	OSO 98	KITT 97
346	18 30 28.88	-17 42 53.4	CB143 B311,L356	Cle	SEST 96	SEST 96
347	18 30 40.82	-16 5 20.5	CB144 L374(?)	Cle	SEST 96	SEST 96
348	18 32 24.39	-9 10 29.7	CB145 B1,L443	Cle	SEST 96	SEST 96

Nr	RA (J2000) h m s	Dec (J2000) ° ′ ″	Name	Cat	Observatory CS (2-1)	Observatory CS (3-2)
349	18 32 32.15	-8 57 44.2	CB146 B101	Cle	SEST 96	SEST 96
350	18 32 52.46	-9 13 49.7	CB147 B1,L443	Cle	SEST 96	SEST 96
351	18 33 18.01	-26 1 33.6	CB148 B98,L239	Cle	SEST 96	SEST 96
352	18 38 8.83	-13 43 58.1	CB149 B102,L401	Cle	SEST 96	SEST 96
353	18 38 55.03	13 23 24.4	CB150	Cle	SEST 97	SEST 97
354	18 39 20.32	13 8 53.2	CB151	Cle	SEST 97	SEST 97
355	18 41 36.19	-2 9 16.7	CB152 B316,L555	Cle	SEST 96	SEST 96
356	18 42 28.63	-19 59 13.7	CB153 B315,L346	Cle	SEST 96	SEST 96
357	18 47 18.94	-4 33 6.3	CB155 B104	Cle	SEST 96	SEST 96
358	18 48 56.54	-5 4 52.3	CB156 B106	Cle	SEST 96	SEST 96
359	18 53 2.70	-6 59 0.9	CB157 B114,L514	Cle	SEST 96	SEST 96
360	18 53 20.32	-6 39 31.6	CB158 B115,L518	Cle	SEST 96	SEST 96
361	18 53 22.45	-6 46 14.5	CB159 SCHO943	Cle	SEST 96	SEST 96
362	18 53 40.20	-7 25 30.2	CB160 B117	Cle	SEST 96	SEST 96
363	18 53 56.22	-7 26 29.1	CB161 B118	Cle	SEST 96	SEST 96
364	18 54 23.97	-7 13 51.1	CB162 SCHO950	Cle	SEST 96	SEST 96
365	18 54 34.90	-4 33 17.2	CB163 B119	Cle	SEST 96	SEST 96
366	18 54 50.95	-4 36 3.1	CB164 B120	Cle	SEST 96	SEST 96
367	18 55 44.77	-4 26 29.3	CB165 B322	Cle	SEST 96	SEST 96
368	18 56 47.12	-4 45 25.9	CB166 B122,L545	Cle	SEST 96	SEST 96
369	18 57 32.10	-4 44 15.7	CB167 B123,L546	Cle	SEST 96	SEST 96
370	18 58 59.87	-4 32 30.5	CB168 B126,L556	Cle	SEST 96	SEST 96
371	18 59 24.83	-4 30 48.7	CB169 B126,L556	Cle	SEST 96	SEST 96
372	19 1 51.33	-36 58 51.9	DC 359.9-17.9	Har	SEST 96	SEST 96
373	19 1 31.89	-5 27 19.8	CB170 B127,L544	Cle	SEST 96	SEST 96
374	19 1 40.88	-4 33 58.1	CB171 B128	Cle	SEST 96	SEST 96
375	19 1 44.78	-5 21 43.9	CB172	Cle	SEST 96	SEST 96
376	19 1 45.99	-5 32 50.8	CB173 B130	Cle	SEST 96	SEST 96
377	19 1 58.01	-5 33 57.0	CB174 B130	Cle	SEST 96	SEST 96
378	19 2 5.70	-5 17 51.4	CB175 B129,L549	Cle	SEST 96	SEST 96
379	19 2 13.67	-4 22 44.8	CB176	Cle	SEST 96	SEST 96
380	19 4 36.75	-5 21 1.8	CB179	Cle	SEST 96	SEST 96
381	19 10 8.42	-78 36 2.5	DC 315.8-27.5	Har	SEST 96	SEST 96
382	19 10 57.12	-78 36 5.1	DC 315.8-27.5	Har	SEST 96	SEST 96
383	19 6 12.48	-6 53 27.2	CB180 B133,L531	Cle	SEST 97	SEST 97
384	19 12 13.12	17 57 50.9	CB182 L714	Cle	SEST 97	SEST 97
385	19 13 20.83	16 34 38.6	CB183	Cle	SEST 97	SEST 97
386	19 13 52.99	16 27 24.8	CB184 L709	Cle	OSO 98	KITT 97
387	19 15 56.19	-1 19 7.4	CB185 B137	Cle	SEST 97	SEST 97
388	19 16 7.14	-1 16 18.6	CB186 B137	Cle	SEST 97	SEST 97
389	19 20 16.83	11 36 12.0	CB188	Cle	OSO 98	KITT 97
390	19 20 30.94	11 30 37.0	CB189 L676	Cle	SEST 97	SEST 97
391	19 20 47.46	23 29 33.6	CB190 L771	Cle	OSO 98	KITT 97
392	19 23 19.95	12 25 51.6	CB192 L686	Cle	SEST 97	SEST 97
393	19 23 51.46	11 7 0.7	CB193 L675	Cle	SEST 97	SEST 97
394	19 26 32.48	23 58 42.2	L778	BM	OSO 98	KITT 97
395	19 29 55.67	14 34 39.5	CB194	Cle	SEST 97	SEST 97
396	19 34 47.44	12 14 30.0	CB195 L701	Cle	SEST 97	SEST 97
397	19 35 15.36	12 19 46.9	CB196 B334	Cle	SEST 97	SEST 97
398	19 36 6.42	18 23 35.5	CB197	Cle	SEST 97	SEST 97
399	19 36 35.40	12 19 39.2	CB198 B336,L702	Cle	SEST 98	no
400	19 37 1.03	7 34 10.8	CB199 B335,L663	Cle	OSO 98	KITT 97
401	19 41 30.73	11 13 59.8	CB200 B143,L7	Cle	SEST 97	SEST 97
402	19 42 10.60	11 22 4.4	CB201 SCHO1080	Cle	SEST 97	SEST 97
403	19 42 31.13	18 52 9.1	CB202	Cle	OSO 98	KITT 97
404	19 43 55.94	19 4 59.6	CB203 SCHO1091(?)	Cle	SEST 97	SEST 97
405	19 44 40.63	8 37 48.2	CB204 L680	Cle	SEST 98	no
406	19 45 27.05	27 52 21.0	CB205 L810	Cle	OSO 97	KITT 97

Nr	RA (J2000) h m s	Dec (J2000) ° ′ ″	Name	Cat	Observatory CS (2-1)	Observatory CS (3-2)
407	19 46 30.51	21 13 31.8	CB207	Cle	OSO 98	KITT 97
408	19 54 40.48	33 47 23.0	CB210 L832	Cle	OSO 97	no
409	19 59 46.80	24 55 29.2	CB211 L802	Cle	OSO 98	KITT 97
410	20 1 31.18	24 42 46.7	CB213 L805	Cle	OSO 98	KITT 97
411	20 3 59.96	26 39 17.2	CB214 L814(?)	Cle	OSO 98	KITT 97
412	20 4 14.83	26 46 1.1	CB215 L814(?)	Cle	OSO 98	KITT 97
413	20 7 6.66	27 28 52.8	IRAS 20050	???	OSO 98	KITT 97
414	20 7 44.82	37 5 53.6	CB217 L863	Cle	OSO 97	no
415	20 18 18.80	63 52 39.4	CB219 LBN444	Cle	OSO 97	no
416	20 23 19.91	68 1 55.0	CB220	Cle	OSO 97	KITT 97
417	20 31 41.99	25 59 51.2	CB221	Cle	OSO 97	no
418	20 33 30.47	64 1 27.8	CB222 L1094	Cle	OSO 97	KITT 97
419	20 34 46.20	64 10 45.1	CB223	Cle	OSO 97	KITT 97
420	20 35 50.18	67 54 22.3	L1152	BM	OSO 97	KITT 97
421	20 36 17.14	63 53 15.2	CB224 L11(?)	Cle	OSO 97	KITT 97
422	20 37 51.42	56 18 19.7	CB225	Cle	OSO 97	KITT 97
423	20 43 29.88	67 52 41.9	L1155C	BM	OSO 97	no
424	20 48 18.17	59 38 21.6	CB226 B148	Cle	OSO 97	KITT 97
425	20 49 18.90	59 31 12.9	CB227 B149	Cle	OSO 97	no
426	20 50 43.14	44 21 59.4	Sug31 HII(S117)	S91	OSO 97	KITT 97
427	20 51 20.41	56 15 45.1	CB228	Cle	OSO 97	KITT 97
428	20 51 27.42	60 18 59.8	L1082C	BM	OSO 97	KITT 97
429	20 53 29.57	60 14 40.3	L1082A	BM	OSO 97	KITT 97
430	20 53 50.28	60 9 46.4	L1082B	BM	OSO 97	KITT 97
431	20 53 32.09	68 18 27.4	CB229 L1171	Cle	OSO 97	KITT 97
432	21 0 22.43	68 12 52.8	L1174	BM	OSO 97	KITT 97
433	21 2 23.97	67 54 7.9	L1172	BM	OSO 97	KITT 97
434	21 12 20.11	47 24 24.1	B361	BM	OSO 98	KITT 97
435	21 17 40.83	68 18 23.0	CB230 L1177	Cle	OSO 97	KITT 97
436	21 32 23.66	57 24 8.3	Sug32 HII(S131)	S91	OSO 98	KITT 97
437	21 33 12.13	57 29 34.4	Sug33 HII(S131)	S91	OSO 98	KITT 97
438	21 33 32.28	58 3 28.3	Sug34 HII(S131)	S91	OSO 97	KITT 97
439	21 33 55.53	54 41 29.2	CB231 B157	Cle	OSO 97	no
440	21 36 5.38	58 31 39.0	Sug35 HII(S131)	S91	OSO 98	KITT 97
441	21 36 12.31	57 27 34.2	Sug36 HII(S131)	S91	OSO 98	KITT 97
442	21 37 13.82	43 21 34.3	CB232 B158	Cle	OSO 98	KITT 97
443	21 40 28.92	56 35 58.0	Sug37 HII(S131)	S91	OSO 98	KITT 97
444	21 40 33.03	57 48 6.2	CB233 B161	Cle	OSO 97	KITT 97
445	21 40 42.27	58 16 9.7	Sug38 HII(S131)	S91	OSO 98	KITT 97
446	21 40 33.40	70 18 33.2	CB234 LBN515	Cle	OSO 97	KITT 97
447	21 46 6.75	57 26 22.9	Sug39 HII(S131)	S91	OSO 98	KITT 97
448	21 46 14.62	57 8 59.2	Sug40 HII(S131)	S91	OSO 98	KITT 97
449	21 46 29.17	57 18 40.8	Sug41 HII(S131)	S91	OSO 98	KITT 97
450	21 46 36.74	57 12 25.1	Sug42 HII(S131)	S91	OSO 98	KITT 97
451	21 47 25.69	47 32 9.7	L1031B	BM	OSO 98	KITT 97
452	21 56 18.45	59 1 9.8	CB235 L1142	Cle	OSO 98	KITT 97
453	22 5 25.10	59 33 32.6	CB236 L1166	Cle	OSO 97	KITT 97
454	22 7 21.70	59 40 14.7	CB237 B173,L1169	Cle	OSO 97	KITT 97
455	22 13 22.48	41 1 31.4	CB238	Cle	OSO 97	KITT 97
456	22 9 56.65	86 44 2.7	CB239	Cle	OSO 97	no
457	22 28 52.15	64 13 43.4	Sug44 HII(S145)	S91	OSO 97	KITT 97
458	22 30 31.70	75 14 16.8	L1251A(2,0)	BM	OSO 97	KITT 97
459	22 31 18.79	75 13 18.1	L1251A(5,-1)	BM	OSO 97	KITT 97
460	22 33 48.34	58 33 30.5	CB240 L1192	Cle	OSO 97	KITT 97
461	22 47 48.74	58 2 50.4	Sug43 HII(S142)	S91	OSO 97	no
462	23 11 41.78	66 3 6.9	CB241 L1239	Cle	OSO 98	KITT 97
463	23 11 57.51	61 39 4.1	CB242 L1225	Cle	OSO 98	KITT 97
464	23 25 12.82	63 36 29.8	CB243 L1246	Cle	OSO 98	KITT 97

Nr	RA (J2000) h m s	Dec (J2000) ° ′ ″	Name	Cat	Observatory CS (2-1)	Observatory CS (3-2)
465	23 25 29.56	74 18 15.0	L1262A	BM	OSO 97	KITT 97
466	23 25 48.71	74 17 37.2	CB244 L1262,L1261	Cle	OSO 97	KITT 97
467	23 55 21.86	58 51 21.7	CB245 SCHO1448	Cle	OSO 97	no
468	23 56 43.54	58 34 28.8	CB246 L1253	Cle	OSO 97	KITT 97
469	23 57 25.32	64 49 26.9	CB247 L1263	Cle	OSO 97	no
470	23 59 25.71	67 23 39.0	Sug1 HII(S171)	S91	OSO 97	KITT 97
471	0 1 49.86	48 6 8.0	CB248	Cle	OSO 98	KITT 97

Catalogue id

BM - Benson & Myers (1989)
Cle - Clemens & Barvainis (1988)
Har - Hartley et al. (1996)
LLM - Larsson et al. (2000)
Lor - Loren et al. (1990)
S91 - Sugitani et al. (1991)